Charles University

Faculty of Science

Study program: Medicinal Chemistry

Katarína Markušová

Syntéza 7-aryl-7-deazapurinových derivátů jako potenciálních inhibitorů MARK4
Synthesis of 7-aryl-7-deazapurines as potential inhibitors of MARK4

Bachelor thesis

Supervisor: Prof. Ing. Michal Hocek, CSc., DSc.

Prague, 2021

Prohlášení

Prohlašuji, že jsem závěrečnou práci zpracovala samostatně a že jsem uvedla všechny použité informační zdroje a literaturu. Tato práce ani její podstatná část nebyla předložena k získání jiného nebo stejného akademického titulu.

V Praze, *16.06.2021*

Katarína Markušová

Acknowledgements

Abstract

In this bachelor thesis, a series of 7-aryl-7-deazapurine derivatives was synthesized from the starting 6-chloro-7-deazapurine by iodination, protection, nucleophilic aromatic substitution, and derivatization by Suzuki cross-coupling followed by deprotection. Optimization of the Suzuki cross-coupling reactions was performed where needed. This way, we

successfully prepared seven compounds that are potential inhibitors of the human MARK4 kinase – an enzyme identified as one of the targets for the treatment of Alzheimer disease (AD).

Key words: *kinase inhibitors, 7-deazapurines, cross-couplings, heterocycles*

Abstrakt

V této bakalářské práci byla z výchozího 6-chlor-7-deazapurinu syntetizována série 7-aryl-7-deazapurinových derivátů za pomoci jodace, nachránění, nukleofilní aromatické substituce, derivatizace Suzukiho cross-coupligovou reakcí a závěrečného odchránění. Pokud to bylo potřebné, byla provedena optimalizace Suzukiho cross-couplingové reakce. Tímto způsobem jsme úspěšně připravili sedm sloučenin, které jsou potenciálními inhibitory lidské MARK4 kinázy – enzymu identifikovaného jako jeden z cílů pro léčbu Alzheimerovy nemoci.

Klíčová slova: *kinázové inhibitory, 7-deazapuriny, cross-couplingy, heterocykly*

Content

List of abbreviations

Aβ – beta amyloid(s)

AD – Alzheimer disease

APCI – atmospheric pressure chemical ionization

cHex – cyclohexane

CDK – cyclin dependent kinase

COSY – correlation spectroscopy

DCM – dichloromethane

DMF – *N,N*-dimethylformamide

DMSO – dimethyl sulfoxide

EtOAc – ethyl acetate

HMBC – heteronuclear multiple bond correlation

HPFC – high pressure fluid chromatography

HR MS (ESI) – high resolution mass spectroscopy (electrospray ionization)

HSQC – heteronuclear single quantum coherence

*i*PrOH – isopropyl alcohol, 2-propanol

IR (ATR) – infrared spectroscopy (attenuated total reflection)

LRRK2 – Leucine-rich repeat kinase 2

MARK4 – Microtubule Affinity Regulating Kinase 4

Me – methyl

m.p. – melting point

MS – mass spectroscopy

NFT – neurofibrillary tangles

NIS – *N*-iodosuccinimide

NMR – nuclear magnetic resonance

R_f – retention factor

SEM – 2-(trimethylsilyl)ethoxymethyl

TFA – trifluoroacetic acid

THF – tetrahydrofuran

TLC – thin layer chromatography

TPPTS – 3,3′,3″-phosphanetriyltris(benzenesulfonic acid) trisodium salt

USFDA – The United States Food and Drug Administration

1. Introduction

Alzheimer disease (AD) is an irreversible neurodegenerative disease that causes progressive memory loss and results in dementia.[1] Even though the death toll of AD is very difficult to correctly estimate, the data from the Centers for Disease Control and Prevention states that in the year 2019 there were over 120 000 casualties in the United States of America for which AD had been determined as the underlying cause of death.[2] The only available treatment so far is symptomatic, it does not manage to cure the disease if it is already in progression, nor can it prevent the outbreak of the disease.[3] There is a need for therapeutics with a new mechanism of action. The enzyme Microtubule Affinity Regulating Kinase 4 (MARK4) has been identified as one of the targets to treat AD.[4,5] To focus on its inhibition may be the path to future AD treatment.

1.1 *Alzheimer disease (AD)*

AD was first described by Alois Alzheimer[6] in 1907 on a case of a 51-year-old woman showing rapid memory deterioration. The disease generally appears mainly among the older part of the population. Its symptoms include progressive memory loss, deterioration of cognitive abilities, impairment of judgement, language disturbance as well as possible seizures and hallucinations.[7] Lack of physical activity, smoking and absence of adequate social contacts are examples of recognized lifestyle-related mid-to-late life modifiable risk factors. A medical background of hypertension, diabetes, depression, severe head traumas or obesity also contributes to the modifiable risk factor count.[8]

AD shows to be the most common cause of dementia, with estimated responsibility for as many as 70 % of the cases (*Figure 1*).[9,10]
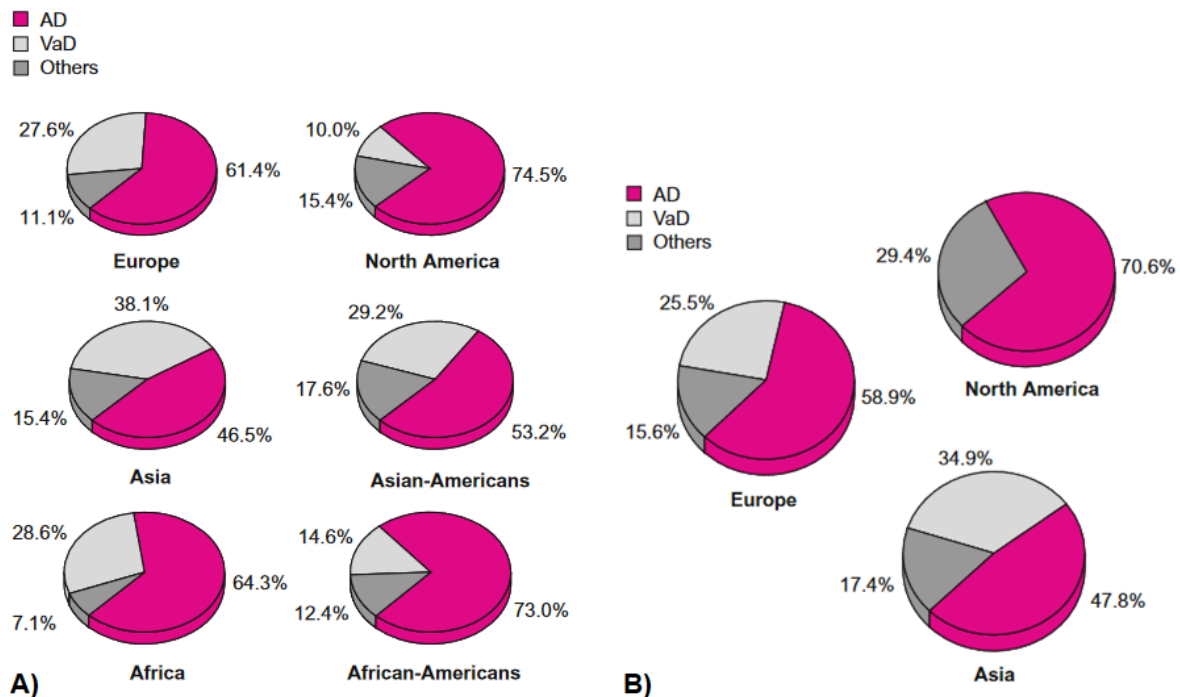
Figure 1 – A) Prevalent dementia cases: proportion of different dementing disorders in different continents. Pooled data from Europe, Asia and North America. **B)** Incident dementia cases: proportion of different dementing disorders in different countries, pooled data from Europe, Asia and the United States of America. AD = Alzheimer's disease; VaD = vascular dementia.[10]

A recent Korean study placed AD as number nine on the "top ten" list of causes of death in the Republic of Korea, specifying that of the dementia related mortality in 2018 (19.0 cases per 100 000 population overall), AD comprised a 63% majority (well in agreement with worldwide estimations). With 12.0 cases per 100 000 population, this falls just shy of 4 000 deaths from AD related dementia in 2018.[11] A Chinese analysis from 2020 reports a prevalence of 3.20 % among population over 60 years of age, based on 99 studies with a total population of 385 312, and predicts the increase rate to almost double in the next 5 years.[12] Latest papers from the United States of America estimate around 6 million Americans to be currently suffering from AD, growing by 360 000 cases each year, with the yearly death toll being consistently around 100 000 people.[13,14] Calculations are predicting the amount of AD patients to rise up to 13.8 million by 2050.[13] Overall prevalence of dementia in Europe reaches 5–7 % (numbers for individual countries differ slightly) by two independent analyses,[15,16] and expects a 40% increase by 2030.[17] Bearing in mind the percentage of dementia cases being ascribed to AD, these findings along with the globally calculated 40 to 50 million people

currently living with dementia[18] are alarming facts. Worldwide mid-century estimations even exceed 100 million people being affected specifically by AD-type dementia. [17,19]

1.1.1 Types of Alzheimer disease

There have been disputes about whether to treat the disease as a single entity, differentiated only from various other possible causes of dementia, or as two forms, namely the early-onset type (described in patients under 65 years of age) and the late-onset type (in patients of 65 years of age and older).[20] Tellechea *et al.*[20] summarize a number of studies about AD and conclude that there are in fact significant differences between the early-onset and the late-onset variant, including typical sites of brain tissue atrophy, poorer performance of certain typical skills and rate of progression. Patients who have the early-onset type of the disease often display atypical clinical presentation of the disease (up to a third of cases). Bearers of the early-onset type also have a more aggressive course of the disease. Compared to the late-onset type, they have poorer performance on complex attention tasks, visual-cognitive tasks and on tasks concerning motor skills and written language. On the other hand, the late-onset type patients perform worse on visual conformation naming tests (e.g. the Boston Naming Test), are more affected by memory loss and exhibit more severe dementia.[20] The late-onset type comprises a vast majority of all AD cases.[21]

Apart from this distinction, AD can also be characterized as either sporadic or familial.[22] The proposed risks for the so-called sporadic variant (without the presence of an inherited genetic mutation) are environmental factors and having one form of the apolipoprotein E (APOE ε4 allele variant)[23] with the chromosome location of 19q13.32[24]. The term familial AD may be used if there is evidence of autosomal dominant inheritance of certain mutations in a particular family; and in most cases it is characterized by early-onset manifestation.[25] Known genetic linkages include defects in genes APP (Aβ protein precursor), PSEN1 (Presenilin 1) and PSEN2 (Presenilin 2).[26] Familial AD was first reported in 1932.[27]

1.1.2 Neuropathological manifestations

AD is associated with several brain tissue alterations. The main causes suggested are (prolonged) oxidative stress, mitochondrial dysfunction, metal ion dysregulation, tissue response to inflammation, beta amyloid accumulation and tau protein hyperphosphorylation. All of them are inherently connected and are influencing each other.[28,29] The combination of all

of these factors leads to neuronal damage and degradation of the synaptic pathways.[30] Two factors that are most commonly presented as the potential crucial mechanisms of AD development and progression – the beta amyloid and the tau protein will be discussed in more detail.

Beta amyloids (amyloid beta, amyloid-β, Aβ) were identified to be the main components of the so-called amyloid plaques which can be found in the brain tissue of AD patients.[31] They are a group of 39 to 42 amino-acid peptides, alternatively spliced from the amyloid precursor protein (APP).[32,33] This happens by the combination of cleavage by the enzymes β-secretase and γ-secretase, instead of the non-pathological cleavage by α-secretase and γ-secretase (**Figure 2**).[30]
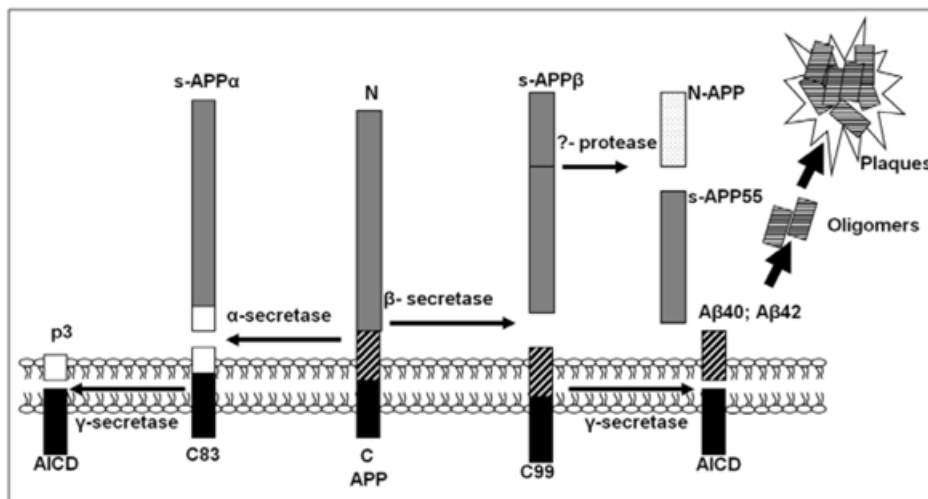
Figure 2 – Alternative splicing of the amyloid precursor protein (APP).[30]

Among the two most common forms of the peptide, Aβ(1-42) and Aβ(1-40),[34] differentiated at the C-terminus by 2 amino-acid residues (I and A),[33] these aggregates consist predominantly of the Aβ(1-42), which is more prone to aggregation than the overall more expressed Aβ(1-40).[35] The reason for this appears to be the greater rigidness[36] and presence of more beta-sheets and hydrophobic surface regions if placed in non-denaturing environment[37]. The atomic structure of Aβ(1-42) as well as 3D models of its monomeric and oligomeric structure have been successfully mapped.[33,38]

Literature overall agrees on the oligomeric form of the amyloid protein (as opposed to the monomeric or polymeric = fibril form) being the most toxic and the most

important in relevance to AD development.[39,40,41] This mechanism of toxicity, known as the amyloid beta oligomer (AβO) hypothesis, has been first suggested in 1998.[42]

Tau protein (tubulin-associated unit protein, τ-protein) belongs to the group of microtubule-associated proteins (MAP) and has multiple known isoforms[43,44] alternatively spliced from the microtubule-associated protein tau (MAPT).[43] It was first described in 1975 by its founders as a "factor associated with tubulin" which promotes its self-assembly into microtubules.[45]

It is physiologically found in all nucleated cells[9] (mainly axon-located)[46] and functions as a stabilizer of microtubules by attachment to the formed tubule (***Figure 3***), the affinity for which is regulated by phosphorylation.[47]
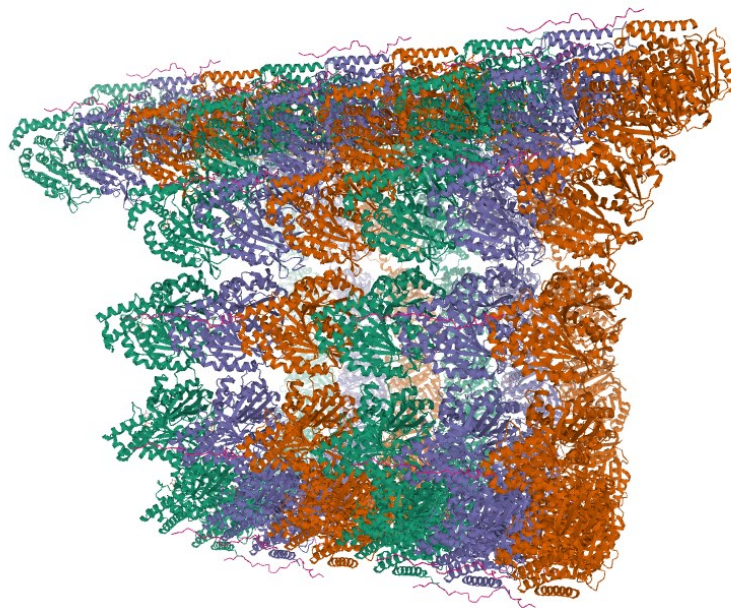
Figure 3 - Model of synthetic tau (R2x4) bound to the microtubule. (PDB code: 6CVN, 3.90 Å resolution).[48]

Upon mutation or hyper-phosphorylation of tau, the affinity of its binding domain for microtubules is lost and so-called neurofibrillary tangles (NFTs) – aggregates of tau filaments – are formed by tau self-assembly into paired helical and/or straight filaments.[49] This results in the disintegration of the cell's microtubular network and the development

of neurodegenerative tauopathies (Pick disease, Down syndrome, Alzheimer disease etc.).[50] Tau protein pathological forms are now considered to act as a major and independent cause of thus formed dementias, as opposed to an older opinion of tau only being a "downstream pathology", secondary to (and promoted by) primary Aβ pathology.[51]

Tau undergoes physiological and, under certain conditions, also pathological phosphorylation by a considerable number of enzymes at numerous amino-acid residues, mainly serines and threonines.[52] The ones most associated with AD-type tauopathies, either as sensitive clinical markers (for differentiation of the diagnosis from non-AD tauopathies) or potential drug targets, are Thr_{181}, Thr_{231} and Ser_{262} (the latter phosphorylated by MARK kinases as mentioned later).[53,54,55,56]

1.1.3 Treatment

Currently, the available medication does not prevent the development of AD, only lessens the symptoms and may mildly slow the progression of the disease.[8] The United States Food and Drug Administration (USFDA) approved medication prescribed for the whole spectrum of severity of AD cases (mild to severe) includes cholinesterase inhibitors donepezil, galantamine and rivastigmine (under the brand names Aricept®, Reminyl®/Razadyne® and Exelon® respectively); and memantine (Namenda®), an N-methyl-D-aspartate receptor (glutamate receptor) blocker. A combination of donepezil and memantine (under the brand name of Namzaric®) is used to treat patients suffering from moderate to severe stages of AD.[8,57] Common side effects throughout the whole spectrum of available medication are nausea, vomiting, diarrhea, dizziness and loss of weight and appetite.[8,57]

1.2 *MARK4*

The Microtubule Affinity Regulating Kinase 4, (also previously referred to as the MARKL1)[58] is a serine/threonine kinase belonging to the MARK protein family.[59] The MARK protein family has previously been reported as belonging to the wider KIN1/PAR-1/MARK kinase family, members of which are yeast-to-human conserved and exhibit similarity in primary structure, though seemingly having widely diverse functions.[47] Along with the other members of the family (MARK1-3), MARK4 is normally expressed mainly in spleen, kidney, and brain tissue.[60]

It has been proven that the MARK family is responsible for the early tau protein phosphorylation at the Ser_{262} residue.[61,62,63] This specific phosphorylation significantly decreases the affinity of the tau protein for microtubule binding,[64,65] which separates it from the microtubule and allows for further phosphorylation. This effectively causes the AD-related NFT formation.[66] Research indicates that MARK4 specifically may play a distinctly important role in tau phosphorylation in association with AD manifestation and pathology.[4,59,67] This correlates with the findings that MARK4 is overexpressed in brains affected by AD.[4] MARK4 therefore shows to be a valid target for anti-AD drug research and development.[5]
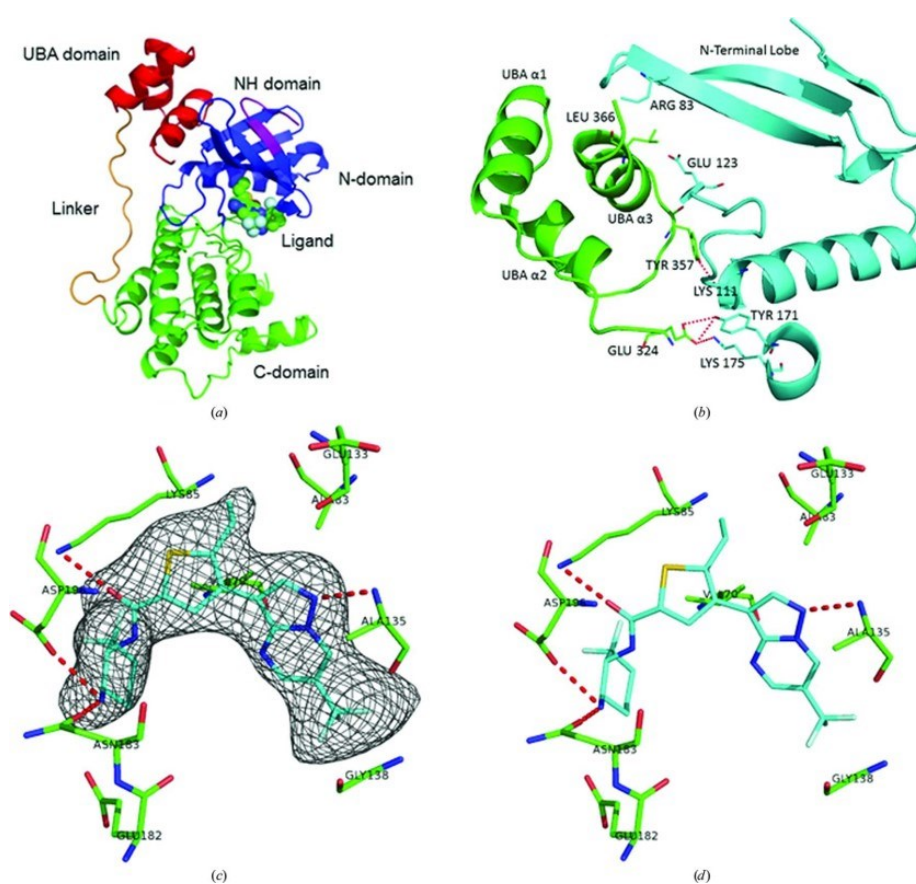
Figure 4 – Structure of the MARK4 complex with a pyrazolopyrimidine inhibitor [(1*R*,6*R*)-6-amino-2,2-difluorocyclohexyl]-5-ethyl-4-{6-(trifluoromethyl)pyrazolo[1,5-a]pyrimidin-3-yl}-2-thiophene-2-carboxamide. (a) Cartoon diagram of the MARK4 structure showing the NH domain (purple), N-domain (blue), C-domain (green), linker (orange) and UBA domain (red) [PDB code: 5ES1, 2.80 Å resolution]. (b) Cartoon diagram of the interaction between the CD (blue) and UBA (green) domains in MARK4. (c) The final Fo − Fc OMIT electron-density map contoured at 2.5 r.m.s.d. is shown with the final model of compound 1 in the ATP-binding site of MARK4. (d) Stick figure of the binding of compound 1 showing the hydrogen-bonding scheme (the drawings were generated using PyMOL). [adopted from Sack *et al.*[68]]

The previous search for MARK4 inhibitors has resulted in the finding of (among other substituted heteroaromatics[69,70]) substituted pyrazolopyrimidines (nitrogen containing aromatic heterocycles) that showed nanomolar inhibitory activity against the enzyme (**Figure 4**, **Figure 5**).[68,71]
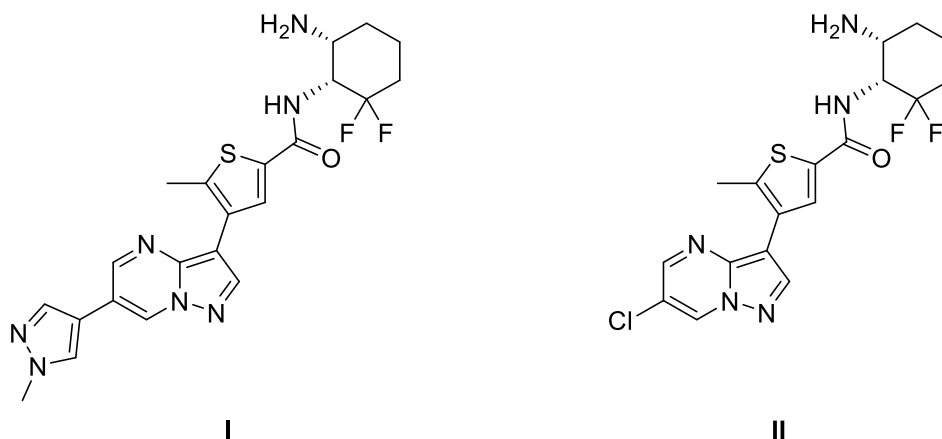
Figure 5 – Examples of pyrazolopyrimidine MARK4 inhibitors.[71]

1.3 Purines, deazapurines

Purines are heterocyclic aromatic compounds derived from the purine molecule which consist of one pyrimidine and one imidazole ring fused together. Among nitrogen-containing heterocycles, they are the ones most frequently found in nature.[72] The two most prominent natural purine derivatives are the adenine (A) and guanine (G) nucleobases (**Figure 6**) as DNA components. Their corresponding nucleotide triphosphates, adenosine triphosphate (ATP) and guanosine triphosphate (GTP) are essential for the function of kinases, enzymes that catalyze the transfer of phosphate groups from one of these high energy molecules onto a substrate (e. g. a protein or a lipid).[73,74] Therefore, kinases inherently possess a binding site for these purine-derived molecules.[73]

Figure 6 – Purine and its most prominent natural derivatives.

There are known artificial purine derivatives that demonstrably function as kinase inhibitors. Seliciclib (roscovitine), olomoucine and bohemine (***Figure 7***) are known inhibitors of cyclin dependent kinases (CDKs).[75,76,77,78] These compounds and their derivatives have already been subjected to clinical trials (phase II – in human trials for seliciclib and its derivatives) with successful results as anticancer agents.[79,80,81,82,83]
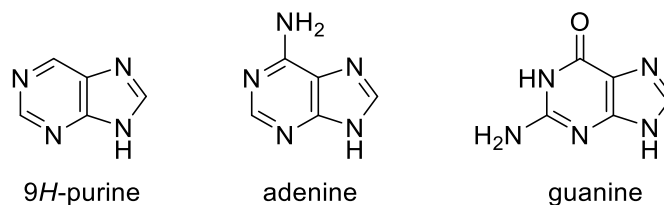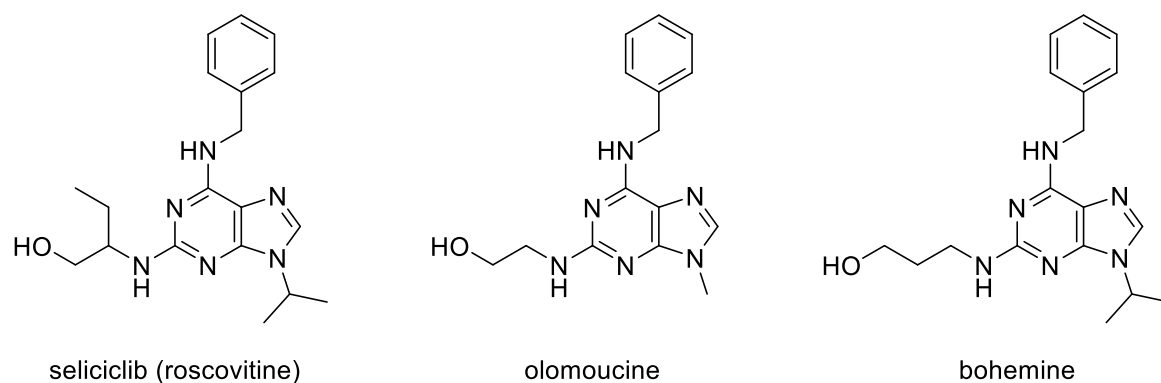

Figure 7 – Selected purine derivatives with known CDK-inhibitory aktivity.[78]

Deazapurines are purine derivatives created by exchanging one of the nitrogen atoms for a CH group. This work focuses on the 7*H*-pyrrolo[2,3-*d*]pyrimidine, or 7-deazapurine, derivatives of which were first isolated from *Streptomyces* bacteria cultures in the early second half of the 20th century,[84,85,86] and can be found in terrestrial as well as in marine species.[87] 7-Deazapurines are generally very potent cytostatics and many of them have been reported to function as inhibitors for a large spectrum of kinases: adenosine kinase,[88] SRC kinase,[89] protein kinase D[90] and others.[91,92,93] The compound **PF-06447475** (***Figure 8***) synthesized by Henderson *et al.*[94] selectively inhibits the LRRK2 kinase. One of our derivatives, **6a**, was previously synthesized by Galatsis *et al.*[95] and it exhibited nanomolar inhibition of the LRRK2 (***Figure 8***).

7H-pyrrolo[2,3-d]pyrimidine
7-deazapurine

PF-06447475

6a

Figure 8 – 7H-pyrrolo[2,3-d]pyrimidine (7-deazapurine) and its derivatives synthesized by Henderson *et al.* (**PF-06447475**)[94] and Galatsis *et al.* (**6a**).[95]

The Hocek research group has experience with the synthesis of diversely substituted 7-deazapurine bases (***Figure 9***).[96,97] Our library of 7-deazapurines contains hundreds of compounds.

X = OMe, SMe, NH$_2$, Me
Y = H, Me, NH$_2$
R = furyl, thienyl, benzofuryl, phenyl

μM cytostatic

inactive

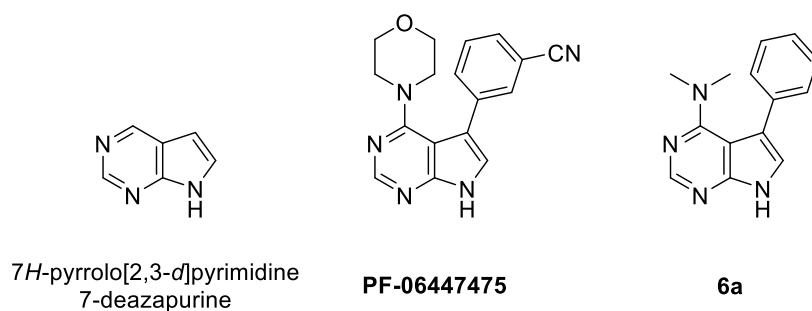X = thienyl, furyl, Me, NH$_2$, NHMe, NMe$_2$, OMe
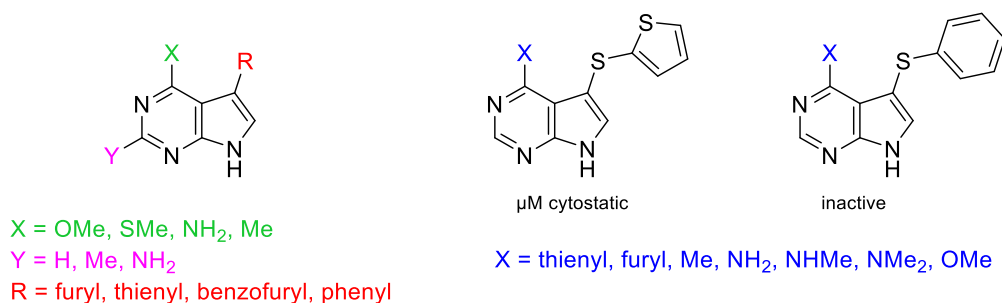
Figure 9 – 7-deazapurine derivatives previously synthesized in the Hocek group.

Recently, the enzyme MARK4 was identified as a promising target to treat AD, and as 7-deazapurine nucleobases have a great potential for inhibition of various kinases, we screened our library of various modified 7-deazapurines for MARK4 inhibition. This original screening identified multiple hits with IC$_{50}$s in single-digit micromolar range, among them, two 6-methoxy-7-deazapurines bearing phenyl (IC$_{50}$ = 0.24 μM) or thiophenyl (IC$_{50}$ = 0.12 μM) group in position 7. Based on these results, we decided to perform SAR study of such type of compounds and we designed several series of 7-deazapurine nucleobases with the aim to study the influence of a small substituent in position 6 (OMe, SMe, NHMe, NMe$_2$, NH$_2$, Me) and to find the best aryl group for substitution in position 7. The target structures were designed by molecular modeling using the Moloc (all-atom MAB force field) software[98] and the only known amd available MARK4 crystal structure (PDB code: 5ES1,

2.80 Å resolution)[99] (**Figure 10**, **Figure 11**). Modeling revealed that there is a potential for creating additional hydrogen bonds with Asp_{196} and Asn_{183}, so the original phenyl ring was replaced by pyridine, aminopyridine, aminophenyl, pyrrole and pyrazole. The goal of this work is to prepare one series of the target compounds, specifically 6-*N*,*N*-dimethylamino-7-deazapurines bearing various aryl groups in position 7 as a first generation MARK4 inhibitors (**Scheme 2**).

Figure 10 – Molecular docking of representative selected 7-deazapurines – **6a** (phenyl) and **6d** (aminophenyl) – in the active site of the enzyme MARK4. Distances of particular nitrogen atoms from their amino-acid residue hydrogen bond partners are shown as dashed black lines and are given in ångströms (Å). Color code: *red* – O; *blue* – N; *green* – C of MARK4; *magenta* – C of **6a**; *orange* – C of **6d**.
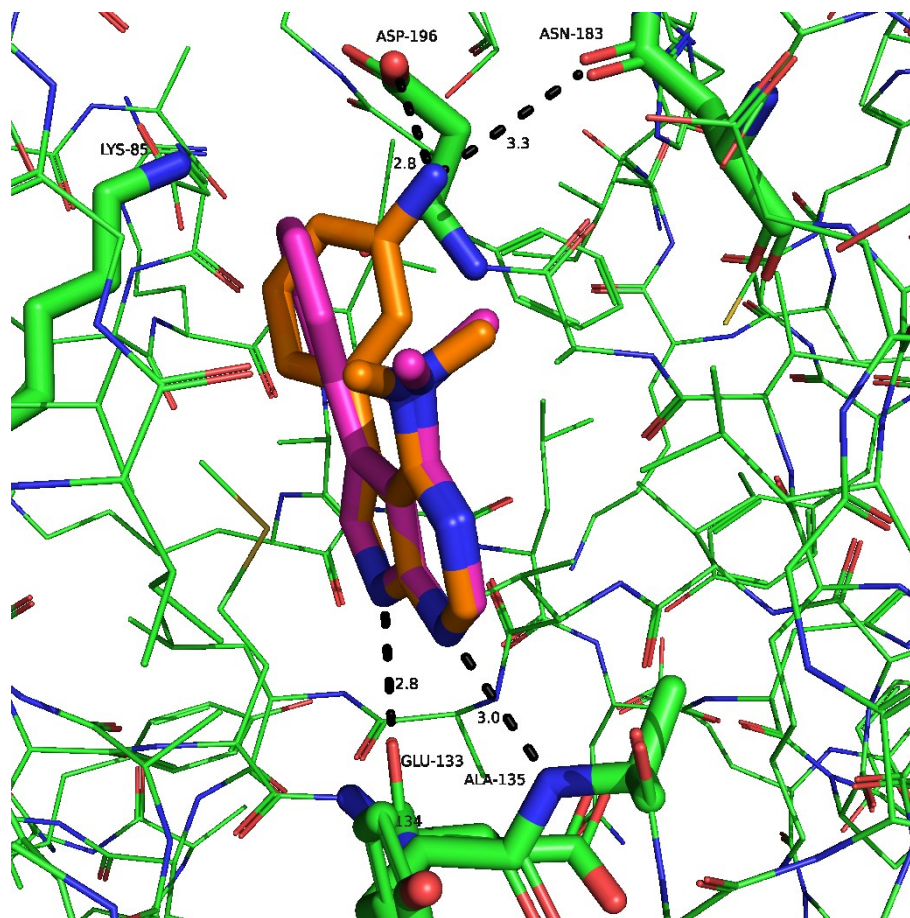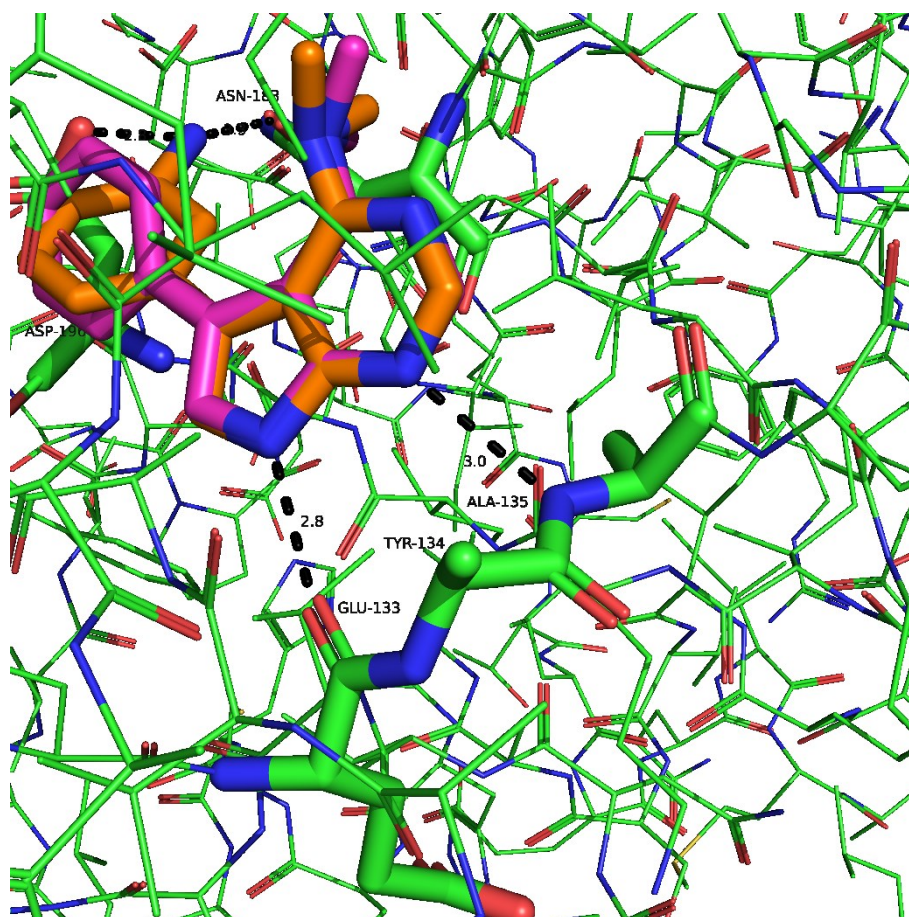
Figure 11 – Molecular docking of representative selected 7-deazapurines – **6a** (phenyl) and **6d** (aminophenyl) – in the active site of the enzyme MARK4. Distances of particular nitrogen atoms from their amino-acid residue hydrogen bond partners are shown as dashed black lines and are given in ångströms (Å). The phenyl ring of Tyr_{134} is omitted for clarity. Color code: *red* – O; *blue* – N; *green* – C of MARK4; *magenta* – C of **6a**; *orange* – C of **6d**.

1.4 *Suzuki-Miyaura cross-coupling reaction*

A key step of the synthesis of the target compounds in this thesis will be derivatization by the Suzuki-Miyaura cross-coupling reaction (also known as Suzuki (cross-)coupling). First published by Suzuki *et al.* in 1979[100], the method describes a palladium catalyzed reaction of an organo-halide with an organoboron species in the presence of a base. This reaction belongs to the group of the cross-coupling reactions with C-C bond formation. The importance of the organic cross-coupling reactions is supported by the fact that the 2010 Nobel Prize in chemistry was jointly awarded to Akira Suzuki, Ei-ichi Negishi and Richard F. Heck "for palladium-catalyzed cross couplings in organic synthesis".[101]

The first step of the Suzuki coupling – the oxidative addition of the organoboron species to the palladium complex – is often the rate-determining step.[102] During this step, palladium

changes its oxidation state from palladium(0) to palladium(II) (***Scheme 1***).[102] All organo-halide species (R[1]-X) form a stable trans-complex with palladium. Inversion of the configuration from cis to trans is observed for the oxidative addition of allyl- and benzyl-halides, but not for alkyl- and alkenyl-halides.[102,103] The second step, which is the transmetalation with the boronic acid (R[2]-B(OH)$_2$), occurs with the retention of the stereochemistry in the complex (***Scheme 1***).[103] The last step, the reductive elimination of the desired product (R[1]-R[2]) – proceeds after isomerization of the trans-complex to its corresponding cis-complex, and with the release of the product from the complex, palladium changes its oxidation state back to palladium(0) (***Scheme 1***).[102]
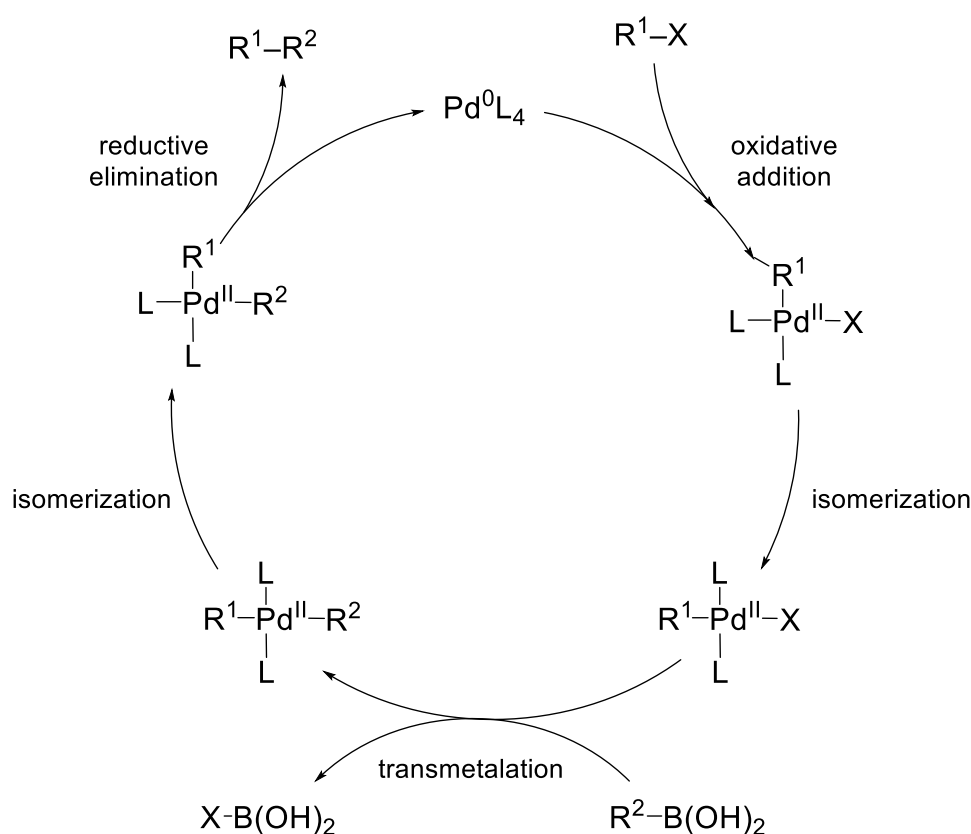
Scheme 1 – The Suzuki-Miyaura coupling catalytic cycle.[104]

The overall rate of the coupling reaction is greatly influenced by the choice of all of the reactants mentioned above. The organoboron species used in the Suzuki cross-coupling reaction is typically a boronic acid or its ester. The organo-halide as the electrophilic partner of the reaction can be any of alkyl, alkenyl, alkynyl, allyl, benzyl or aryl moiety. Among

the possible halides (the halide functions as a leaving group), iodine is overall the most reactive in Suzuki cross-coupling reactions (***Figure 12***).[103,105] The presence of electron-withdrawing groups makes the organo-halide species more prone to the oxidative addition to the palladium complex.[102]

$$I \gg Br \gg Cl$$
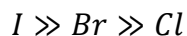
Figure 12 – The order of reactivity of the electrophilic partner based on the choice of the leaving group.[105]

The base used in the reaction is suggested to be involved in the transmetalation process.[103] Weaker bases (such as phosphates or carbonates) were found to work better when DMF is used as a solvent for the reaction. Stronger bases (such as NaOH or NaOMe) produced more successful results in a THF/H_2O solvent mixture.[106] Palladium catalysts are widely used for Suzuki cross-coupling reactions. Here, palladium is in the form of a complex with a certain number of (preferably) bulky, electron-rich ligands – this makes the catalyst more stable and reactive.[107] Some of the most commonly used palladium catalysts include Pd(dppf)Cl$_2$, Pd(PPh$_3$)$_4$, Pd$_2$(dba)$_3$ or Pd(OAc)$_2$ with TPPTS (*in situ* complex formation).[102,103,106,108,109]

2. Aim of the project

The aim of this bachelor project is to synthetize a series of 6,7-disubstituted 7-deazapurines as potential MARK4 inhibitors. Position 6 will have a stable substituent (dimethylamine), while the substituents chosen for position 7 will include 5- and 6-member aromatic cycles containing up to 2 nitrogen atoms and in some cases bearing an attached amino group. The synthesized compounds will be submitted for biological testing to determine their inhibitory activity against MARK4, where we aim to determine whether and how the nature of the selected substituents will influence the activity of the compounds.

3. Results and discussion

3.1 *Synthesis of target 7-substituted 6-N,N-dimethylamino-7-deazapurines*

We aimed to prepare six 6,7-disubstituted 7-deazapurines as our target compounds (*Scheme 2*).
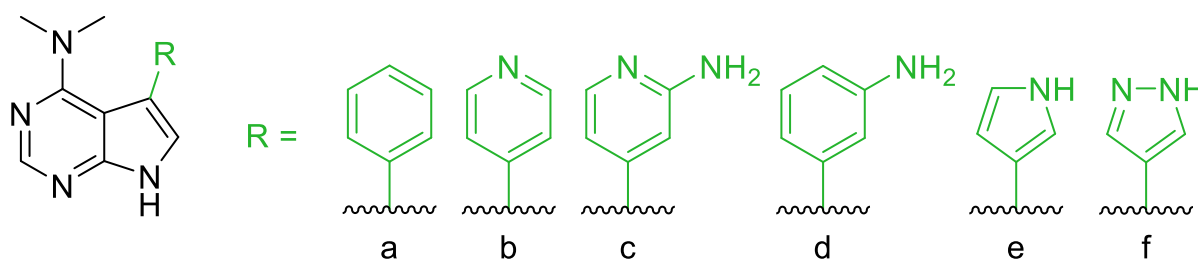
Scheme 2 – A series of six proposed 6-*N,N*-dimethylamino-7-deazapurine derivatives.

A five-step synthetic plan of the 7-substituted 6-*N,N*-dimethylamino-7-deazapurines was designed (*Scheme 3*), starting from the commercially available 6-chloro-7-deazapurine (**1**).
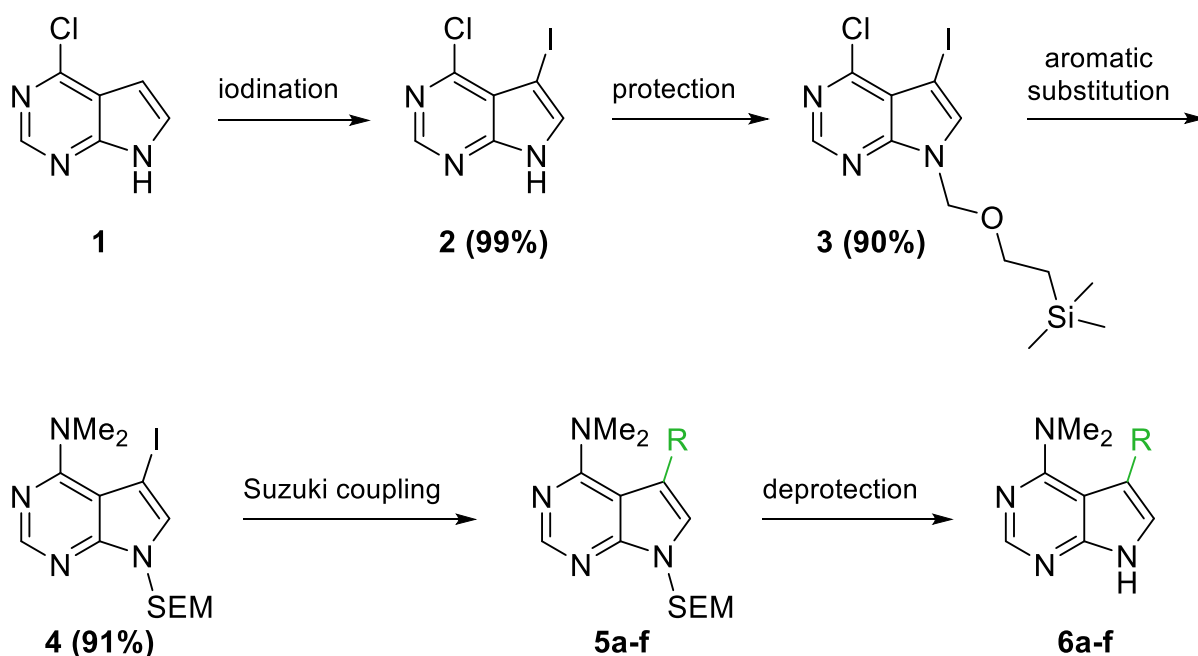
Scheme 3 – The plan for synthesis of the target 7-substituted 6-*N,N*-dimethylamino-7-deazapurines.

6-Chloro-7-deazapurine (**1**) was first iodinated in position 7 by *N*-iodosuccinimide in DMF according to a published procedure[110] to produce compound **2** in 99% yield. In the second step, compound **2** was protected at the pyrrolic nitrogen by a 2-(trimethylsilyl)ethoxymethyl (SEM) protecting group according to a modified published procedure using SEM-Cl and NaH in DMF,[111] giving compound **3** with a 90% yield. Compound **3** was then subjected to aromatic substitution. A dimethylamino group was introduced to position 6 of the molecule via a published procedure using Me₂NH in *i*PrOH,[112] resulting in compound **4** with a 91% yield. The fourth step was a Suzuki coupling reaction in position 7 with six different substituents to prepare compounds **5a-f**. This will be later discussed in more detail. The last step was the deprotection of the pyrrolic nitrogen by TFA in DCM and subsequent treatment with aqueous ammonia in MeOH according to a published procedure,[97] yielding the final products **6a-f**.

3.1.1 Suzuki cross-coupling

Derivatization in position 7 was performed by Suzuki cross-coupling reactions with the corresponding R-boronic acids (**Scheme 4**). Protected boronic acids were used where needed.
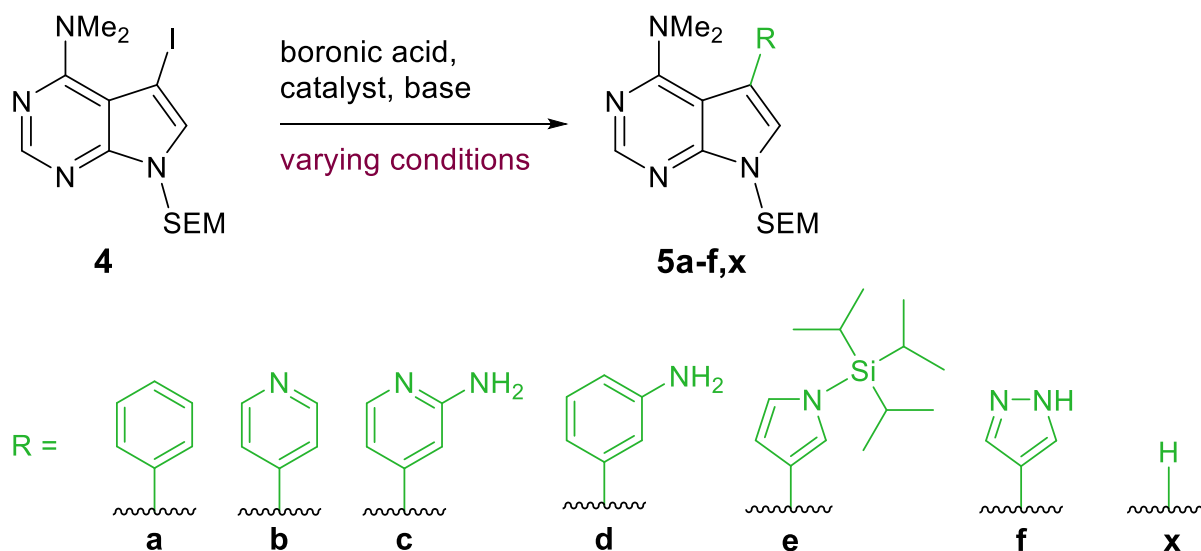
Scheme 4 – Derivatization of compound **4** by the Suzuki coupling reaction in position 7.

Initially, compound **4** was subjected to Suzuki coupling with substituent **a** according to a published procedure, which was previously successfully applied for the synthesis

of 2,6,7-trisubstituted-7-deazapurines.[97] 1 equivalent of **1** along with 1.5 equivalents of phenylboronic acid, 3 equivalents of Na_2CO_3, 0.05 equivalents of $Pd(OAc)_2$, and 0.125 equivalents of TPPTS in H_2O/MeCN (2:1) were stirred at 100 °C for 4 h. The derivative **5a** was successfully isolated as the only product of the reaction with a yield of 44%, which we later tried to improve.

Next, compound **4** was subjected to Suzuki coupling with substituents **b**, **c**, **d** and **e** under modified conditions of the previously mentioned procedure[97] – Cs_2CO_3 was used as the base and the equivalents of the base, $Pd(OAc)_2$ and TPPTS were doubled in an attempt to achieve better yield of the desired products. Unfortunately, this procedure only successfully worked for derivative **5e**, which was isolated as the only product of the reaction with a yield of 43%, which we later also tried to improve. The couplings with substituents **b**, **c** and **f** all gave only a deiodinated side product **5x** in yields up to 62% (***Table 2***, ***Table 3***, ***Table 5***, Entry 1). This comes as no surprise, because dehalogenation is often the undesired competing reaction for the palladium-catalyzed cross-couplings.[113,114]

Because only two of the coupling reactions worked under either the published conditions[97] (phenyl **5a)** or their modification (pyrrole **5e**), we decided to change the conditions for the rest of the compounds and we also tried to improve the yield of **5a** and **5e**.

3.1.2 Optimization of Suzuki cross-coupling reactions

For the second attempt of the synthesis of derivative **5a**, the successful reaction conditions from attempt 1 were repeated with only the change of the solvent ratio from 2:1 to 1:2 H_2O/MeCN in order to improve the solubility of the not very hydrophilic starting material (***Table 1***, Entry 2). Again, the reaction gave **5a** as the only product, this time in an improved yield of 85% (***Scheme 5***).
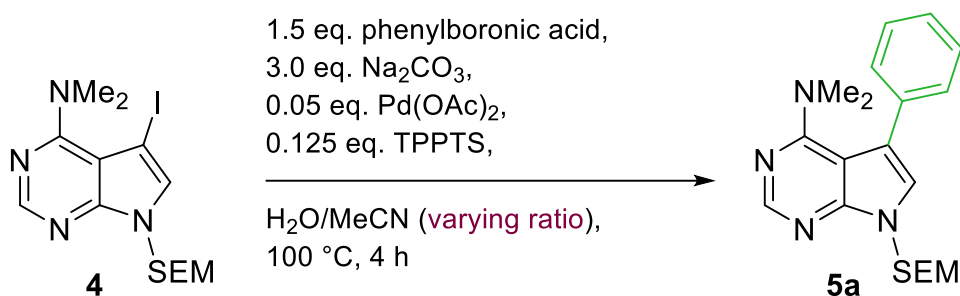
Scheme 5 – Synthesis of compound **5a**.

Table 1 – Reaction optimization for compound **5a**.

Entry	Solvent	Yield of 5a
1	H_2O/MeCN 2:1	44
2	H_2O/MeCN 1:2	85

For the second attempt to synthesize compound **5b**, we again decided to change the solvent system to H_2O/MeCN (1:2) (**Table 2**, Entry 2). However, this only lowered the conversion of the starting material and thus the yield of the deiodinated side product **5x**, but again no desired product **5b** was formed. In the third attempt to synthesize **5b**, new reaction conditions using a different palladium catalyst[115] and DMF as a solvent were applied (**Table 2**, Entry 3). This time the reaction gave **5b** as the only product in a very good yield of 95% (**Scheme 6**). As these conditions worked successfully for the pyridine derivative **5b**, they were later also applied for the synthesis of **5c**, **5d** and **5f**.
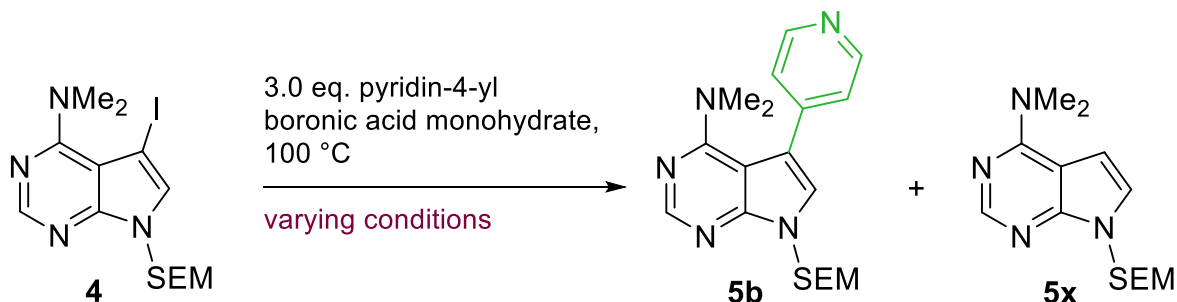
Scheme 6 – Synthesis of compound **5b**.

Table 2 – Reaction optimization for compound **5b**.

Entry	Cs$_2$CO$_3$ [eq.]	Catalyst [eq.]	Lignad [eq.]	Solvent	Time [h]	Yield of 5b [%]	Yield of 5x [%]
1	6	Pd(OAc)$_2$ 0.1	TPPTS 0.25	H$_2$O/MeCN 2:1	19	0	62
2	3	Pd(OAc)$_2$ 0.05	TPPTS 0.125	H$_2$O/MeCN 1:2	5	0	38
3	6	Pd(dppf)Cl$_2$ 0.1	–	DMF	1	95	0

We changed the H$_2$O/MeCN ratio from 2:1 to 1:2 also for the second attempt to synthesize compound **5c** (*Table 3*, Entry 2). Only the deiodinated side product **5x** was formed in the reaction, with a 61% yield. For the third attempt, the conditions that were meanwhile successfully used for the synthesis of **5b** (*Table 2*, Entry 3) were applied. This time, the reaction successfully gave the desired product **5c**, along with the deiodinated side product **5x** (31%) (*Scheme 7*). The attempt to purify the product **5c** was unsuccessful. The unpurified product **5c** in a mixture with **5x** obtained from the reaction was instead used without further purification in the final step of the synthesis. The yield of the last (deprotection) step of the aminopyridine derivative **6c** is therefore calculated over two steps.
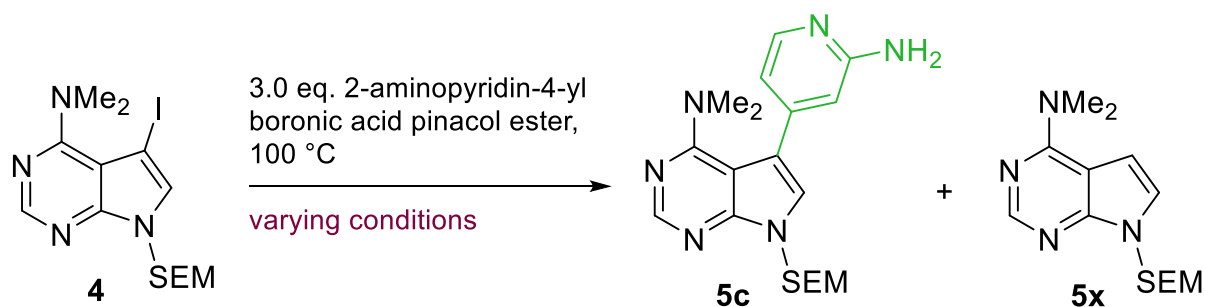

Scheme 7 – Synthesis of compound **5c**.

Table 3 – Reaction optimization for compound **5c**.

Entry	Cs$_2$CO$_3$ [eq.]	Catalyst [eq.]	Lignad [eq.]	Solvent	Time [h]	Yield of **5c** [%]	Yield of **5x** [%]
1	6	Pd(OAc)$_2$ 0.1	TPPTS 0.25	H$_2$O/MeCN 2:1	19	0	–[a]
2	3	Pd(OAc)$_2$ 0.05	TPPTS 0.125	H$_2$O/MeCN 1:2	5	0	61
3	6	Pd(dppf)Cl$_2$ 0.1	–	DMF	5	52[b]	31

[a] not determined, [b] not pure, used without further purification

In an attempt to optimize the synthesis of derivative **5e**, the H$_2$O/MeCN ratio was changed to 1:2 for the second reaction (**Table 4**, Entry 2). This reaction gave the desired compound **5e** along with the deiodinated side product **5x**, but the purification was unsuccessful. The yield of **5e** for this reaction was estimated from the weight of the combined **5e/5x** fraction and the peaks area ratio of the ^{1}H NMR of the **5e/5x** fraction as less than 30%. Because this change in reaction conditions showed unhelpful, the reaction was repeated a third time, using the same equivalents of reactants as the first successful reaction, only changing the solvent ratio (**Table 4**, Entry 3). Product **5e** was obtained from the reaction with a yield of 31%, but this time (compared to the first successful reaction) also the deiodinated side product **5x** (19%) was formed. We concluded that the original reaction conditions showed the most successful as they led to the formation of the desired product **5e** specifically, with no deiodinated side product observed (**Scheme 8**).
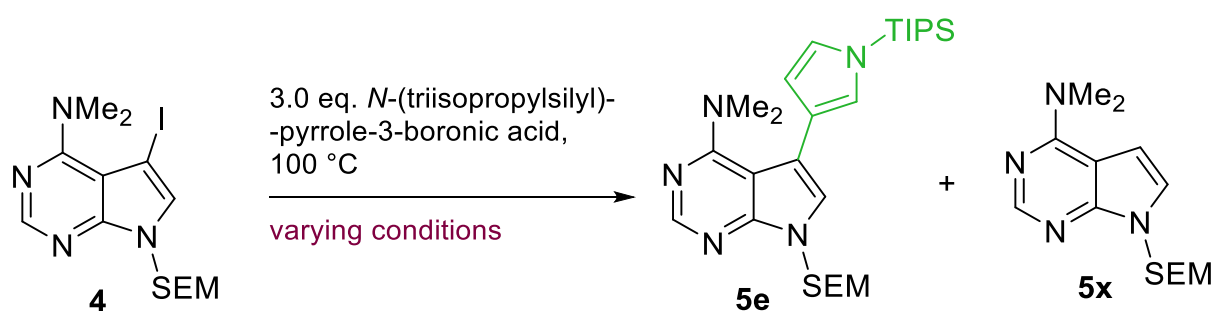
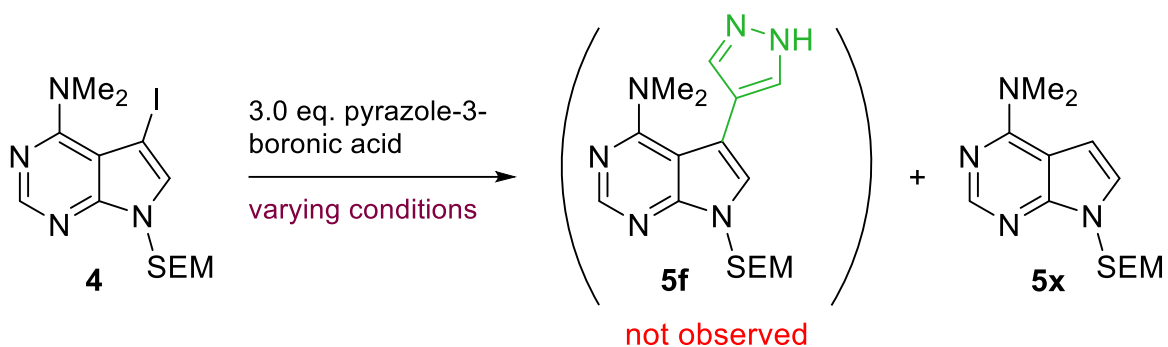*Scheme 8* – Synthesis of compound **5e**.

Table 4 – Reaction optimization for compound **5e**.

Entry	Cs_2CO_3 [eq.]	$Pd(OAc)_2$ [eq.]	TPPTS [eq.]	Solvent	Time [h]	Yield of **5e** [%]	Yield of **5x** [%]
1	6	0.1	0.25	H_2O/MeCN 2:1	24	43	0
2	3	0.05	0.125	H_2O/MeCN 1:2	4	<30[a]	–[a]
3	6	0.1	0.25	H_2O/MeCN 1:2	6	31	19

[a] inseparable

All attempts to synthesize the pyrazole derivative **5f** failed (***Scheme 9***). The first three attempts were performed using the same conditions that were used for the attempts to synthesize the pyridine (**5b**) and aminopyridine (**5c**) derivatives (***Table 2***, ***Table 3***, ***Table 5***, Entry 1-3). All of them were unsuccessful, giving only the deiodinated side product **5x** in various yields (***Table 5***, Entry 1-3). A combination of the previously used 2:1 H_2O/MeCN ratio and $Pd(dppf)Cl_2$ as the catalyst was applied for the fourth attempt. A different catalyst, $Pd(PPh_3)_4$, was applied for the fifth attempt (***Table 5***, Entry 4 and 5). Again, no product **5f** was formed in either of the two reactions (determined by TLC-MS). Presence of the deiodinated side product **5x** was detected by TLC-MS in the crudes of both reactions, and they were combined for separation to determine the combined **5x** yield, which was 65%. Next, for the sixth attempt, we tried to use a different base (K_3PO_4) and solvent (DMF/H_2O 5:1) under the conditions according to a published procedure[116] (***Table 5***, Entry 6). TLC-MS of the reaction mixture showed the presence of the deiodinated side product **5x**, but not the desired product **5f**. Separation in order to determine the yield of **5x** was not performed. For the seventh attempt, the conditions that were successful for derivatives **5b** and **5c** were applied again, but the equivalents of Cs_2CO_3 were lowered to 2 and the reaction temperature was lowered to 60 °C (in an attempt to see whether the amount of base used or the high temperatures do not cause the boronic acid to decompose). No conversion of the starting material whatsoever was observed in the reaction (***Table 5***, Entry 7).

Scheme 9 – Synthesis of compound **5f**.

Table 5 – Attempts for the synthesis of compound **5f**.

Entry	Base [eq.]	Catalyst [eq.]	TPPTS [eq.]	Solvent	Temp. [°C]	Time [h]	Yield of 5f [%]	Yield of 5x [%]
1	Cs$_2$CO$_3$ 6	Pd(OAc)$_2$ 0.1	0.25	H$_2$O/MeCN 2:1	100	24	0	47
2	Cs$_2$CO$_3$ 3	Pd(OAc)$_2$ 0.05	0.125	H$_2$O/MeCN 1:2	100	4	0	traces
3	Cs$_2$CO$_3$ 6	Pd(dppf)Cl$_2$ 0.1	–	DMF	100	48	0	33
4	Cs$_2$CO$_3$ 6	Pd(dppf)Cl$_2$ 0.1	–	H$_2$O/MeCN 2:1	100	24	0	65[a]
5	Cs$_2$CO$_3$ 6	Pd(Ph$_3$P)$_4$ 0.1	–	H$_2$O/MeCN 2:1	100	24	0	65[a]
6	K$_3$PO$_4$ 4	Pd(dppf)Cl$_2$ 0.1	–	DMF/ H$_2$O 5:1	130	14	0	–[b]
7	Cs$_2$CO$_3$ 2	Pd(dppf)Cl$_2$ 0.1	–	DMF	60	24	0	0

[a] entry 4 and 5 were separated together, [b] not determined

We tried to reverse the steps four and five (Suzuki coupling and deprotection) to synthesize the pyrazole derivative. Compound **4** was therefore subjected to the deprotection reaction. We expected the deprotection to lead to the formation of 4-*N*,*N*-dimethylamino-5-iodo-7*H*-pyrrolo[2,3-*d*]pyrimidine that could be subjected to Suzuki coupling, but instead both deprotection and deiodination happened simultaneously and the result was the 4-*N*,*N*-dimethylamino-7*H*-pyrrolo[2,3-*d*]pyrimidine (compound **6x**). Particular reaction conditions and yield of the reaction are stated in the next chapter (***Scheme 12***). We treated compound **6x** as a final product and subjected it to biological testing.

To determine the possible reason behind the Suzuki couplings with the pyrazole-3-boronic acid not working, the coupling was performed on a different substrate

(2-amino-4-iodopyridine) under conditions according to Entry 3 in **Table 5**. After 3.5 h, the reaction has not proceeded at all (**Scheme 10**).

3.0 eq. pyrazole-3-boronic acid,
6.0 eq. Cs_2CO_3,
0.1 eq. $Pd(dppf)Cl_2$,
DMF, 100 °C, 3.5 h
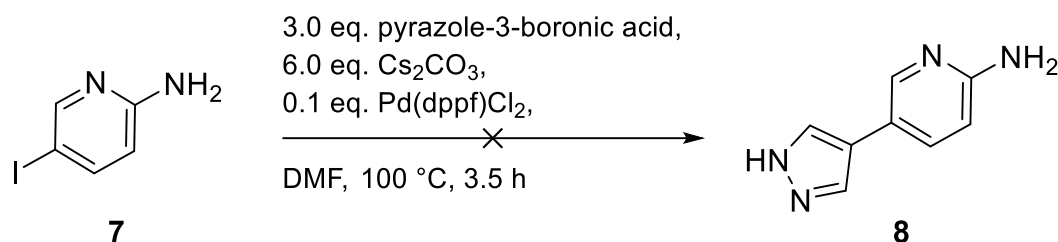
Scheme 10 – Synthesis of 2-amino-5-(3-pyrazolo)-pyrimidine.

We concluded that there might be a problem with the boronic acid itself. The use of a pyrazole-protected boronic acid should be considered in the future. Any further attempts to synthesize compound **5f** will also need to consider an optimization of the reaction conditions.

The last target compound was the aminophenyl derivative (**5d**). For its synthesis, the conditions previously used for the successful synthesis of pyridine and aminopyridine derivatives (**5b** and **5c**) were applied (**Table 2**, **Table 3**, Entry 3). The reaction immediately gave the desired product **5d** in a yield of 88% (**Scheme 11**).

3.0 eq. 3-aminophenyl boronic acid,
6.0 eq. Cs_2CO_3,
0.1 eq. $Pd(dppf)Cl_2$,
DMF, 100 °C, 1 h
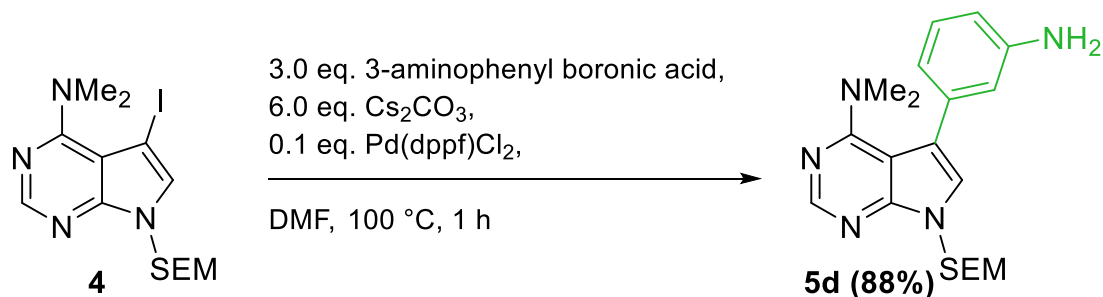
Scheme 11 – Synthesis of compound **5d**.

3.1.3 Deprotection

The last step of the synthesis was the removal of the protecting SEM group from the pyrrolic nitrogen of the deazapurine moiety (for derivative **5e** also the simultaneous removal of the TIPS protecting group from the substituent in position 7). The final products were obtained by using TFA in DCM followed by treatment with aqueous ammonia in MeOH according to a published procedure (**Scheme 12**).[97]
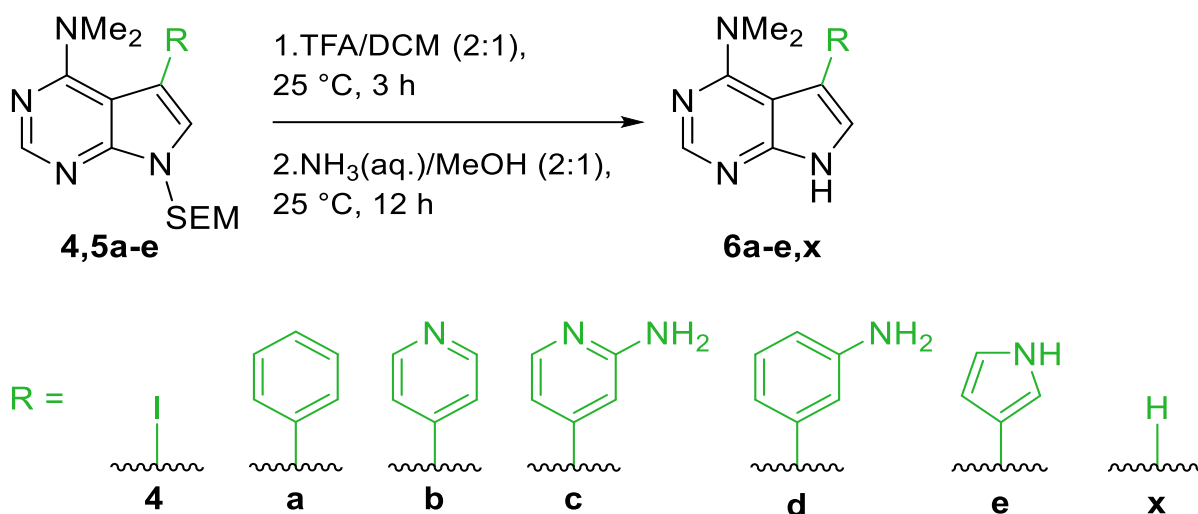
Scheme 12 – Deprotection of the target 7-substituted 6-*N,N*-dimethylamino-7-deazapurines.

Yields of the reactions are summarized in **Table 6**. For the pyridine derivative, the separation yielded the product in two fractions in both the form of a free base (**6b**) and its salt with TFA (**6by**). Both of these compounds were subjected to biological testing. For the aminopyridine derivative (**6c**), the yield is calculated over two steps (Suzuki coupling and deprotection) as mentioned before.

Table 6 – Yields of the final compounds.

Compound	Yield [%]
6a	91
6b	34
6by	60
6c	15
6d	56
6e	29
6x	52

3.2 *Biological activities*

The final compounds were tested for inhibitory activity against the MARK4 enzyme (***Table 7***). All of them except derivative **6x** exhibit sub-micromolar inhibitory activity (derivative **6x** exhibits micromolar inhibitory activity). The best activity was found for compound **6d** (aminophenyl derivative), the worst activity for compound **6x** (7-unsubstituted derivative). The difference between the activities of 7-substituted compounds (**6a-e**, **6by**) versus the 7-unsubstituted compound **6x** is significant – this shows that the presence of a substituent in position 7 is important for the inhibition, as it helps the binding of the compound into the active site of the enzyme by creating additional interactions with the nearby amino-acid residues.

Our most active compound (**6d**, IC_{50} = 34.2 nM) showed to have better inhibitory activity of MARK4 than some of the previously published inhibitors (Shen *et. al.*, derivative **50**, IC_{50} = 1.301±0.102 µM).[117] We therefore conclude that the 6-dimethylamino-7-substituted 7-deazapurine is a promising leading structure for future optimization.

Testing of the final compounds for cytotoxicity on several leukemia and cancer cell lines and for antiviral activities against several viruses is currently in progress.

Table 7 – MARK4 inhibitory activity of the final compounds.

Compound	IC_{50} (µM)
6a	0.0481
6b	0.4323
6by	0.4107
6c	0.1380
6d	0.0342
6e	0.0860
6x	8.7937

4. Conclusion

Out of the six 6,7-disubstituted 7-deazapurines proposed on the basis of molecular modeling and docking, five compounds were successfully prepared (**6a-e**), along with a salt of one of them (**6by**) and a compound deiodinated in the position 7 (**6x**). The synthesized compounds were submitted for biological testing in order to determine their potential inhibitory activity against the MARK4 enzyme, which has been identified as one of the prime targets to treat AD. All of the tested compounds with the exception of compound **6x** exhibit promising inhibitory activities in the sub-micromolar range. We found that the presence of a substituent in position 7 serves to form one or more hydrogen bonds with the amino-acids in the active site of the enzyme. Our results open the possibilities for future research of active 6,7-disubstituted 7-deazapurines as potent kinase inhibitors.

5. Experimental part

5.1 *General remarks*

All reagents and solvents were purchased from commercially available sources and used without further purification. All reactions were performed under argon atmosphere. Reaction monitoring was performed by thin-layer chromatography (TLC) on Merck silica gel 60 F$_{254}$ aluminum sheets and visualized by UV light (λ_{max} = 254 nm or 312 nm). High performance flash chromatography (HPFC) was performed on a *Combi Flash Rf* instrument from *Teledyne Isco Inc.* using SiO$_2$ (particle size 0.040–0.063 mm, 230–400 mesh) from Merck in refillable flash columns, RediSep Rf Gold Silica Gel disposable column or PuriFlash C18-HP 30 μm column. ^{1}H and ^{13}C NMR spectra were measured by Kateřina Bártová at IOCB Prague on a *Bruker Avance III^{TM} HD 500 MHz* spectrometer (at 500.0 MHz and 125.7 MHz respectively) or on a *Bruker Avance III^{TM} HD 600 MHz* (at 600.0 MHz and 150.9 MHz respectively). Chemical shifts (δ) are given in ppm downfield from tetramethyl silane (TMS) internally referenced to residual solvent signal (CDCl$_3$: δ_H = 7.26 ppm, δ_C = 77.00 ppm; DMSO-d_6: δ_H = 2.50 ppm, δ_C = 39.70 ppm). Coupling constants (J) are given in Hz and the multiplets are reported as s (singlet), d (doublet), t (triplet), q (quartet), p (pentet), m (multiplet), and b (broad), or combinations thereof. ^{13}C NMR experiments were performed using APT pulse sequence. DFQ-COSY, HSQC and HMBC experiments were used to assign the ^{1}H and ^{13}C NMR signals where required. Melting points were measured on a *Stuart SMP40* automatic melting point apparatus and are uncorrected. Infrared spectra (IR) were recorded on a *Bruker ALPHA FT-IR* spectrometer using attenuated total reflection (ATR). The spectra of the compounds were measured at 25 °C in their initial state of appearance, absorption bands are reported in wavenumbers ($\tilde{v}$) in the range between 4000–600 cm^{-1}. Intensities are described as strong (s), medium (m) and weak (w). High-resolution mass spectrometry (HR-MS) was performed by the MS-Service at IOCB Prague on a *LTQ Orbitrap XL* instrument from *Thermo Fisher Scientific* using electrospray ionization (ESI) or atmospheric pressure chemical ionization (APCI). Analytical HPLC purity analysis of all final nucleosides (>95%) was carried out using a Waters assembly equipped with a model 600 Controller pump and a model 2996 Photodiode Array Detector. Measurements were performed with a Phenomenex Gemini 5 μm C18 110 Å column of 250 × 4.60 mm, flow rate 1 mL/min. Individual methods are written under the table with HPLC purity. The injector was a model 717 plus Waters Autosampler (10 μL). UV detection was employed. Linear gradients were used in all methods. Run time was 50 min. The acquisition and treatment of data were made with the Empower Pro software.

Biological activity testing of the final compounds was done by *Carna Biosciences, Inc.* The compounds were tested for the inhibition of MARK4 with the use of the Off-chip Mobility Shift Assay (MSA) kit according to the following procedure: 1) The 4× Substrate/ATP/Metal solution was prepared with kit buffer (20 mM HEPES, 0.01% Triton X-100, 5 mM DTT, pH 7.5), and 2× kinase solution was prepared with assay buffer (20 mM HEPES, 0.01% Triton X-100, 1 mM DTT, pH 7.5). 2) The 5 µL of 4× compound solution, 5 µL of 4× Substrate/ATP/Metal solution, and 10 µL of 2× kinase solution were mixed and incubated in a well of polypropylene 384 well microplate for 1 hour at room temperature. 3) 70 µL of Termination Buffer (QuickScout Screening Assist MSA; Carna Biosciences) was added to the well. 4) The reaction mixture was applied to the LabChip^{TM} system (Perkin Elmer), and the product and substrate peptide peaks were separated and quantified. 5) The kinase reaction was evaluated by the product ratio recalculation from peak heights of product (P) and substrate (S) peptides (P/(P+S)).

5.2 *General procedures*

GP1 (Deprotection) – The starting material (**4**, **5a-e**) in TFA/DCM (2:1, 1.5–3 mL) was stirred at 25 °C for 3 h. The reaction mixture was evaporated and co-evaporated with MeOH (3 × 5 mL). Then it was stirred in NH_3(aq.)/MeOH (2:1, 1.5–3 mL) for 12 h, evaporated and co-evaporated with MeOH (3 × 5 mL).

5.3 *Synthetic procedures*

4-Chloro-5-iodo-7*H*-pyrrolo[2,3-*d*]pyrimidine (2)[118]
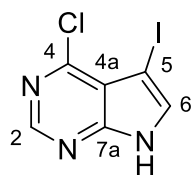
A solution of 4-chloro-7*H*-pyrrolo[2,3-*d*]pyrimidine (**1**) (10.03 g, 65.291 mmol) and NIS (15.08 g, 69.79 mmol) in DMF (100 mL) was stirred at 25 °C for 16 hours. The resulting mixture was poured over ice and left to precipitate in the fridge overnight. The precipitate was filtered, washed with cold water and dried *in vacuo*, giving **2** (18.11 g, 99%) as a pale brown powder.

R_f = 0.49 (SiO$_2$; cHex/EtOAc 2:1); NMR corresponds well with previously published literature[118]; HR MS (ESI) for $C_6H_4N_3ClI^+$ [M + H]$^+$: calcd 279.9133, found 279.9133.

4-Chloro-5-iodo-7-{[2-(trimethylsilyl)ethoxy]methyl}-7*H*-pyrrolo[2,3-*d*]pyrimidine (3)[118]
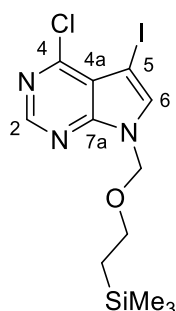
A solution of **2** (8.09 g, 28.96 mmol) in DMF (160 mL) was treated with NaH (1.75 g, 60 wt% suspension in mineral oil, 43.75 mmol) and stirred at 25 °C for 30 min. SEM-Cl (7.18 mL, 40.58 mmol) was added while stirring and the mixture was further stirred for 2 hours at 25 °C. The resulting mixture was treated with water (300 mL) and extracted with EtOAc (3 × 200 mL). The combined organic phases were dried over Na_2SO_4 and concentrated *in vacuo*. Purification by flash chromatography (SiO$_2$; cHex/EtOAc, gradient 0→20% EtOAc) gave **3** (10.64 g, 90%) as a white solid.

R_f = 0.67 (SiO$_2$; cHex/EtOAc 3:1); NMR corresponds well with previously published literature[118]; (HR MS (ESI) for $C_{12}H_{18}N_3OClISi^+$ [M + H]$^+$: calcd 409.9947, found 409.9945.

4-*N*,*N*-Dimethylamino-5-iodo-7-{[2-(trimethylsilyl)ethoxy]methyl}-7*H*-pyrrolo[2,3-*d*]pyrimidine (4)
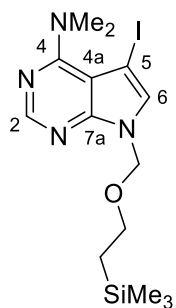
A solution of **3** (2.99 g, 7.30 mmol) in *i*PrOH (150 mL) was treated with Me$_2$NH (9.15 mL, 2M in THF, 18.30 mmol) and stirred at 60 °C for 48 h. Purification by HPFC (SiO$_2$; cHex/EtOAc, gradient 0→50% EtOAc) gave **4** (2.80 g, 91%) as a pale-yellowish solid.

R_f = 0.70 (SiO$_2$; cHex/EtOAc 2:1); ^{1}H NMR (600 MHz, DMSO-d_6): δ = –0.09 (s, 9H; Si*Me₃*), 0.81 (m, 2H; C*H₂*Si), 3.17 (s, 6H; N*Me₂*), 3.50 (m, 2H; OC*H₂*), 5.50 (s, 2H; NC*H₂*O), 7.73 (s, 1H; H-6), 8.26 ppm (s, 1H; H-2); ^{13}C NMR (150.9 MHz, DMSO-d_6): δ = –1.24 (Si*Me₃*), 17.26 (*C*H₂Si), 43.21 (N*Me₂*), 53.26 (C-5), 65.80 (O*C*H₂), 72.36 (N*C*H₂O), 106.11 (C-4a), 132.40 (C-6), 150.69 (C-2), 152.16 (C-7a), 160.24 ppm (C-4); HR MS (ESI) for $C_{14}H_{24}N_4IOSi^+$ [M + H]$^+$: calcd 419.0759, found 419.0760; for $C_{14}H_{23}N_4IONaSi^+$ [M + Na]$^+$: calcd 441.0578, found 441.0579.

4-*N*,*N*-Dimethylamino-5-phenyl-7-{[2-(trimethylsilyl)ethoxy]methyl}-7*H*-pyrrolo[2,3-*d*]pyrimidine (5a)
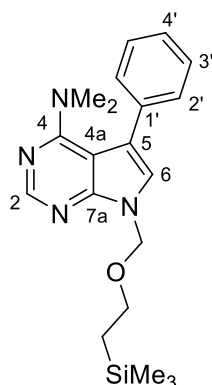
A mixture of **4** (500.3 mg, 1.20 mmol), phenylboronic acid (230.6 mg, 1.80 mmol), Na_2CO_3 (382.3 mg, 3.61 mmol), $Pd(OAc)_2$ (13.5 mg, 0.06 mmol) and TPPTS (89.5 mg, 0.15 mmol) in H_2O/MeCN (2:1, 10 mL) was stirred at 100 °C for 4 h. The resulting mixture was treated with H_2O (200 mL) and saturated NH_4Cl (50 mL) and extracted with MeCN (3 × 200 mL). The combined organic phases were dried over $MgSO_4$ and concentrated *in vacuo*. Purification by HPFC (SiO_2; cHex/EtOAc, gradient 0→50% EtOAc) gave **5a** (374.2 mg, 85 %) as a yellow oil.

R_f = 0.66 (SiO_2; cHex/EtOAc 2:1); ^{1}H NMR (600 MHz, DMSO-d_6): δ = –0.08 (s, 9H; Si*Me$_3$*), 0.84 (m, 2H; C*H$_2$*Si), 2.74 (s, 6H; N*Me$_2$*), 3.57 (m, 2H; OC*H$_2$*), 5.57 (s, 2H; NC*H$_2$*O), 7.31 (m, 1H; H-4'), 7.40–7.48 (m, 4H; H-2' and H-3'), 7.53 (s, 1H; H-6), 8.30 ppm (s, 1H; H-2); ^{13}C NMR (150.9 MHz, DMSO-d_6): δ = –1.23 (Si*Me$_3$*), 17.31 (*C*H$_2$Si), 40.81 (N*Me$_2$*), 65.74 (O*C*H$_2$), 72.54 (N*C*H$_2$O), 101.83 (C-4a), 116.97 (C-5), 124.44 (C-6), 126.55 (C-4'), 128.23 (2C; C-2' or C-3'), 128.69 (2C; C-3' or C-2'), 135.89 (C-1'), 150.64 (C-2), 152.52 (C-7a), 160.17 ppm (C-4); HR MS (ESI) for $C_{20}H_{29}N_4OSi^+$ [M + H]$^+$: calcd 369.2105, found 369.2106; for $C_{20}H_{28}N_4ONaSi^+$ [M + Na]$^+$: calcd 391.1925, found 391.1925.

4-*N*,*N*-Dimethylamino-5-(pyridin-4-yl)-7-{[2-(trimethylsilyl)ethoxy]methyl}-7*H*-pyrrolo[2,3-*d*]pyrimidine (5b)
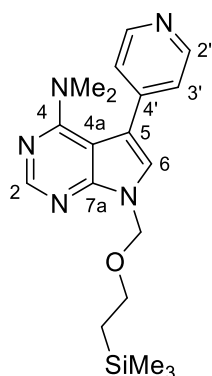
A mixture of **4** (100.8 mg, 0.24 mmol), pyridin-4-yl boronic acid monohydrate (106.7 mg, 0.72 mmol), Cs_2CO_3 (472.5 mg, 1.44 mmol) and $Pd(dppf)Cl_2$ (17.6 mg, 0.02 mmol) in DMF (3 mL) was stirred at 100 °C for 3 h. The resulting mixture was co-evaporated with toluene (3 × 10 mL). Purification by HPFC (SiO_2; cHex/EtOAc, gradient 10→100% EtOAc) gave **5b** (72.8 mg, 82%) as a caramel-brown oil.

R_f = 0.12 (SiO_2; cHex/EtOAc 1:1); ^{1}H NMR (500 MHz, CDCl$_3$): δ = –0.05 (s, 9H; Si*Me$_3$*), 0.93 (m, 2H; C*H$_2$*Si), 2.87 (s, 6H; N*Me$_2$*), 3.60 (m, 2H; OC*H$_2$*), 5.64 (s, 2H; NC*H$_2$*O), 7.38 (s, 1H; H-6), 7.57 (m, 2H; H-2'), 8.48 (s, 1H; H-2), 8.63 ppm (m, 2H; H-3'); ^{13}C NMR (125.7 MHz, CDCl$_3$): δ = –1.47 (Si*Me$_3$*), 17.75 (*C*H$_2$Si),

41.23 (N*Me₂*), 66.82 (O*CH₂*), 73.15 (N*CH₂O*), 101.98 (C-4a), 115.09 (C-5), 123.03 (2C; C-3'), 125.39 (C-6), 145.96 (C-4'), 147.22 (2C; C-2'), 151.64 (C-2), 153.50 (C-7a), 160.74 ppm (C-4); HR MS (ESI) for $C_{19}H_{28}N_5OSi^+$ [M + H]$^+$: calcd 370.2058, found 370.2058.

4-*N*,*N*-Dimethylamino-5-(2-aminopyridin-4-yl)-7-{[2-(trimethylsilyl)ethoxy]methyl}-7*H*-pyrrolo[2,3-*d*]pyrimidine (5c)
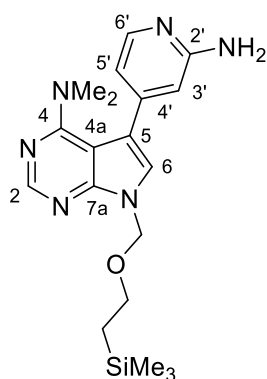

The compound was prepared twice.

1. A mixture of **4** (102.4 mg, 0.25 mmol), 2-aminopyridin-4-yl boronic acid pinacol ester (167.7 mg, 0.72 mmol), Cs₂CO₃ (478.2 mg, 1.45 mmol) and Pd(dppf)Cl₂ (17.7 mg, 0.02 mmol) in DMF (3 mL) was stirred at 100 °C for 5 h. The resulting mixture was co-evaporated with toluene (3 × 5 mL), dissolved in EtOAc and filtered over Celite, then co-evaporated with toluene again (3 × 5 mL).

2. A mixture of **4** (100.9 mg, 0.24 mmol), 2-aminopyridine-4-yl boronic acid pinacol ester (165.3 mg, 0.71 mmol), Cs₂CO₃ (512.1 mg, 1.56 mmol) and Pd(dppf)Cl₂ (18.1 mg, 0.02 mmol) in DMF (3 mL) was stirred at 100 °C for 21 h. The resulting mixture was dissolved in H₂O (50 mL) and extracted by EtOAc (8 × 50 mL).

Attempts for purification of the product were unsuccessful in both cases. Due to difficulties with separation, the combined unpurified product **5c** was directly used in the deprotection step.

HR MS (ESI) for $C_{19}H_{29}N_6OSi^+$ [M + H]$^+$: calcd 385.2167, found 385.2167.

## 4-N,N-Dimethylamino-5-(3-aminophenyl)-7-{[2-(trimethylsilyl)ethoxy]methyl}-7H-pyrrolo[2,3-d]pyrimidine (5d)
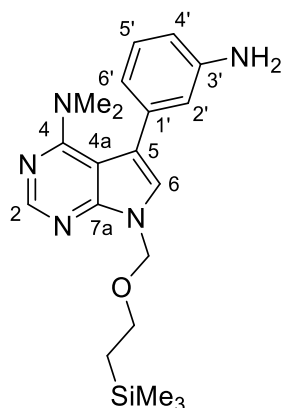
A mixture of **4** (261.3 mg, 0.62 mmol), 3-aminophenylboronic acid (263.3 mg, 1.83 mmol), Cs_2CO_3 (725.1 mg, 2.20 mmol) and $Pd(dppf)Cl_2$ (44.1 mg, 0.06 mmol) in DMF (7.5 mL) was stirred at 100 °C for 1 h. Purification by HPFC (SiO_2; cHex/EtOAc, gradient 0→100% MeOH) gave **5d** (211.1 mg, 88%) as a yellow oil.

R_f = 0.52 (SiO$_2$; cHex/EtOAc 1:2); ^{1}H NMR (600 MHz, DMSO-d_6): δ = −0.09 (s, 9H; SiMe_3), 0.83 (m, 2H; CH_2Si), 2.78 (s, 6H; NMe_2), 3.55 (m, 2H; OCH_2), 5.11 (bs, 2H; NH_2), 5.55 (s, 2H; NCH_2O), 6.50 (ddd, $J_{4',5'}$ = 8.0 Hz, $J_{4',2'}$ = 2.2 Hz, $J_{4',6'}$ = 1.0 Hz, 1H; H-4'); 6.55 (m, 1H; H-6'); 6.65 (m, 1H; H-2'); 7.04 (t, $J_{5',6'}$ = 7.9 Hz, 1H; H-5'); 7.36 (s, 1H; H-6), 8.26 ppm (s, 1H; H-2); ^{13}C NMR (150.9 MHz, DMSO-d_6): δ = −1.19 (SiMe_3), 17.33 (*C*H$_2$Si), 40.70 (NMe_2), 65.67 (O*C*H$_2$), 72.48 (N*C*H$_2$O), 101.74 (C-4a), 112.41 (C-4'), 113.84 (C-2'), 116.25 (C-6'), 117.94 (C-5), 123.62 (C-6), 129.09 (C-5'), 136.58 (C-1'), 148.90 (C-3'), 150.50 (C-2), 152.33 (C-7a), 159.95 ppm (C-4); HR MS (ESI) for $C_{20}H_{30}N_5OSi^+$ [M + H]$^+$: calcd 384.2214, found 384.2215.

4-N,N-Dimethylamino-5-(N-triisopropylsilyl-3-pyrrolo)-7-{[2-(trimethylsilyl)methyl}-7H-pyrrolo[2,3-d]pyrimidine (5e)
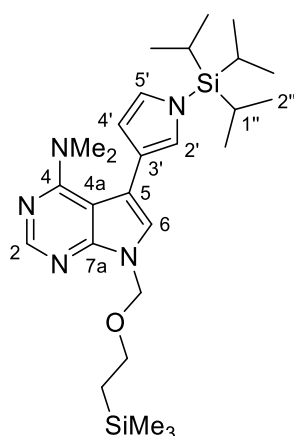
A mixture of **4** (101.2 mg, 0.24 mmol), N-(triisopropylsilyl)pyrrole-3-boronic acid (201.7 mg, 0.72 mmol), Cs_2CO_3 (467.5 mg, 1.44 mmol), $Pd(OAc)_2$ (5.4 mg, 0.02 mmol) and TPPTS (44.7 mg, 0.07 mmol) in H_2O/MeCN (2:1, 1.5 mL) was stirred at 100 °C for 24 h. The resulting mixture was treated with H_2O (100 mL) and saturated NH_4Cl (50 mL) and extracted with DCM (3 × 100 mL). The combined organic phases were dried over $MgSO_4$ and concentrated *in vacuo*. Purification by HPFC (SiO$_2$; cHex/EtOAc, gradient 0→50% EtOAc) gave **5e** (53.8 mg, 43%) as a yellow oil.

R_f = 0.68 (SiO$_2$; cHex/EtOAc 2:1); ^{1}H NMR (500 MHz, DMSO-d_6): δ = −0.09 (s, 9H; SiMe_3), 0.83 (m, 2H; CH_2Si), 1.07 (d, $J_{2'',1''}$ = 7.5 Hz, 18H; H-2''), 1.49 (p, $J_{1'',2''}$ = 7.5 Hz, 3H; H-1''), 2.79

(s, 6H; N*Me₂*), 3.53 (m, 2H; OC*H₂*), 5.53 (s, 2H; NC*H₂*O), 6.35 (dd, $J_{4',2' \text{ or } 5'}$ = 2.5 Hz, $J_{4',5' \text{ or } 2'}$ = 1.5 Hz, 1H; H-4'); 6.84–6.87 (m, 2H; H-2' and 5'); 7.32 (s, 1H; H-6), 8.25 ppm (s, 1H; H-2); ^{13}C NMR (125.7 MHz, DMSO-d_6): δ = –1.22 (Si*Me₃*), 11.12 (3C; C-1''), 17.31 (*C*H₂Si), 17.81 (6C; C-2''), 40.39 (N*Me₂*), 65.55 (O*C*H₂), 72.26 (N*C*H₂O), 103.24 (C-4a), 113.35 (C-5), 111.79 (C-4'), 120.25 (C-3'), 122.04 (C-2' or C-5'), 123.08 (C-6), 124.58 (C-5' or C-2'), 150.22 (C-2), 152.05 (C-7a), 160.72 ppm (C-4); HR MS (ESI) for $C_{27}H_{48}N_5OSi_2^+$ [M + H]$^+$: calcd 514.3392, found 514.3391.

4-*N,N*-Dimethylamino-5-phenyl-7*H*-pyrrolo[2,3-*d*]pyrimidine (6a)[95]
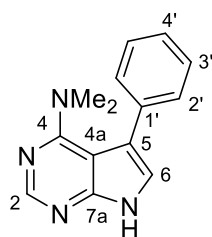
Compound **5a** (198.4 mg, 0.54 mmol) was subjected to GP1. Purification by HPFC (SiO₂; cHex/EtOAc, gradient 0→100% EtOAc) gave **6a** (116.2 mg, 91%) as a pale-beige solid.

R_f = 0.11 (SiO₂; cHex/EtOAc 2:1); m.p. = 198–200 °C; ^{1}H NMR (500 MHz, DMSO-d_6): 2.72 (s, 6H; N*Me₂*), 7.28 (m, 1H; H-4'), 7.35 (d, $J_{6,NH}$ = 2.3 Hz, 1H; H-6), 7.40 (m, 2H; H-3'), 7.46 (m, 2H; H-2'), 8.24 (s, 1H; H-2), 11.97 ppm (bs, 1H; N*H*); ^{13}C NMR (125.7 MHz, DMSO-d_6): 40.88 (N*Me₂*), 101.72 (C-4a), 116.52 (C-5), 121.45 (C-6), 126.15 (C-4'), 128.28 (2C; C-2'), 128.57 (2C; C-3'), 136.48 (C-1'), 150.36 (C-2), 153.02 (C-7a), 160.23 ppm (C-4); IR (ATR, neat): $\tilde{v}$ = 2920 (w), 2849 (w), 1555 (m), 1498 (m), 1399 (m), 1224 (m), 1054 (m), 920 (m), 854 (m), 814 (m), 759 (s), 700 (s), 624 cm^{-1} (s); HR MS (ESI) for $C_{14}H_{15}N_4^+$ [M + H]$^+$: calcd 239.1291, found 239.1292.

4-*N,N*-Dimethylamino-5-(pyridin-4-yl)-7*H*-pyrrolo[2,3-*d*]pyrimidine (6b)
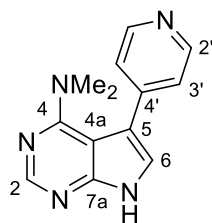
Compound **5b** (98.9 mg, 0.27 mmol) was subjected to GP1. Purification by HPFC (SiO₂; DCM/MeOH, gradient 0→10% MeOH) gave **6b** in both the form of a **base** (**6b**, 22.1 mg, 35%) as an off-white solid and its **TFA salt** (**6by**, 57.8 mg, 60%) as a pale-brown solid.

6b: R_f = 0.35 (SiO₂; EtOAc/MeOH 10:1); m.p. = 245–247 °C; ^{1}H NMR (500 MHz, DMSO-d_6): δ = 2.78 (s, 6H; N*Me₂*), 7.50 (m, 2H; H-3'), 7.65 (s, 1H; H-6), 8.29 (s, 1H; H-2), 8.55 (m, 2H; H-2'), 12.24 ppm (bs, 1H; N*H*); ^{13}C NMR (125.7 MHz, DMSO-d_6): δ = 41.01 (N*Me₂*), 101.42 (C-4a), 113.92 (C-5), 122.61 (C-3'), 123.71 (C-6), 143.54 (C-4'), 149.76 (C-2'), 150.78 (C-2), 153.56 (C-7a), 160.41 ppm (C-4); IR (ATR, neat): $\tilde{v}$ = 2945 (w), 2803 (w), 2711 (w), 1585 (m), 1562 (m), 1500 (m), 1413 (w), 1400 (m), 1291 (w), 1227 (w),

1142 (w), 1057 (m), 923 (m), 856 (m), 818 (s), 797 (m), 726 (w), 637 cm^{-1} (s); HR MS (ESI) for $C_{13}H_{14}N_5^+$ [M + H]$^+$: calcd 240.1244, found 240.1243.

6by: R_f = 0.35 (SiO$_2$; EtOAc/MeOH 10:1); m.p. = decomposition at >218 °C; ^{1}H NMR (500 MHz, DMSO-d_6): δ = 2.78 (s, 6H; NMe_2), 7.51 (m, 2H; H-3'), 7.67 (d, $J_{6,NH}$ = 2.6 Hz, 1H; H-6), 8.29 (s, 1H; H-2), 8.56 (m, 2H; H-2'), 12.26 ppm (bs, 1H; NH); ^{13}C NMR (125.7 MHz, DMSO-d_6): δ = 41.01 (NMe_2), 101.42 (C-4a), 113.87 (C-5), 122.64 (C-3'), 123.84 (C-6), 143.75 (C-4'), 149.55 (C-2'), 150.79 (C-2), 153.58 (C-7a), 160.41 ppm (C-4); IR (ATR, neat): $\tilde{v}$ = 2945 (w), 2853 (w), 1584 (m), 1563 (m), 1500 (m), 1413 (m), 1400 (m), 1226 (m), 1142 (m), 1057 (m), 856 (m), 817 (s), 796 (s), 624 cm^{-1} (s). HR MS (ESI) was already measured for **6b**.

4-*N,N*-Dimethylamino-5-(2-aminopyridin-4-yl)-7*H*-pyrrolo[2,3-*d*]pyrimidine (6c)
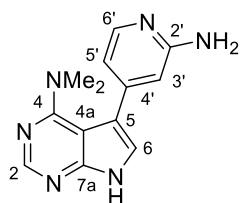
Combined crude product of **5c** was subjected to GP1. Purification by HPFC (SiO$_2$; EtOAc/MeOH, gradient 0→5% MeOH) and repurification (C-18; H$_2$O/MeOH, gradient 5→100% MeOH) gave **6c** (18.8 mg, 15% over two steps) as an off-white solid.

R_f = 0.22 (SiO$_2$; EtOAc/MeOH 10:1); m.p. = 216–218 °C; ^{1}H NMR (500 MHz, DMSO-d_6): δ = 2.82 (s, 6H; NMe_2), 6.53 (m, 1H; H-3'), 6.60 (dd, $J_{5',6'}$ = 5.3 Hz, $J_{5',3'}$ = 1.5 Hz, 1H; H-5'), 7.41 (d, $J_{6,NH}$ = 2.1 Hz, 1H; H-6), 7.88 (d, $J_{6',5'}$ = 5.2 Hz, 1H; H-6'), 8.24 (s, 1H; H-2), 12.04 ppm (bs, 1H; NH); ^{13}C NMR (125.7 MHz, DMSO-d_6): δ = 40.84 (NMe_2), 101.28 (C-4a), 106.54 (C-3'), 112.10 (C-5'), 115.11 (C-5), 122.13 (C-6), 144.63 (C-4'), 147.80 (C-6'), 150.55 (C-2), 153.24 (C-7a), 160.10 (C-4 or C-2'), 160.17 ppm (C-2' or C-4); IR (ATR, neat): $\tilde{v}$ = 3191 (w), 3108 (w), 2921 (w), 2850 (w), 1564 (s), 1504 (m), 1402 (s), 1298 (m), 1228 (m), 1138 (m), 1061 (s), 856 (m), 794 (s), 632 (s), 611 cm^{-1} (s); HR MS (ESI) for $C_{13}H_{15}N_6^+$ [M + H]$^+$: calcd 255.1353, found 255.1353.

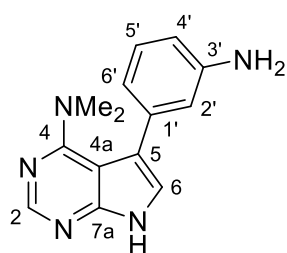### 4-*N,N*-Dimethylamino-5-(3-aminophenyl)-7*H*-pyrrolo[2,3-*d*]pyrimidine (6d)
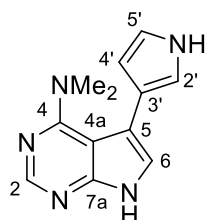

Compound **5d** (211.1 mg, 0.55 mmol) was subjected to GP1. Purification by HPFC (C-18; H$_2$O/MeOH, gradient 5→100% MeOH) gave **6d** (78.3 mg, 56%) as a pearly-white foam.

R_f = 0.48 (SiO$_2$; EtOAc/MeOH 10:1); m.p. = 118–120 °C; ^{1}H NMR (600 MHz, DMSO-d_6): δ = 2.77 (s, 6H; NMe_2), 5.06 (bs,

2H; N*H₂*), 6.48 (ddd, $J_{4',5'}$ = 8.0 Hz, $J_{4',2'}$ = 2.2 Hz, $J_{4',6'}$ = 0.9 Hz, 1H; H-4'); 6.57 (m, 1H; H-6'); 6.66 (m, 1H; H-2'); 7.02 (t, $J_{5',4'}$ = $J_{5',6'}$ = 7.7 Hz, 1H; H-5'); 7.18 (d, $J_{6,NH}$ = 2.4 Hz, 1H; H-6), 8.19 (s, 1H; H-2), 11.81 ppm (bs, 1H; N*H*); ¹³C NMR (150.9 MHz, DMSO-*d₆*): δ = 40.74 (N*Me₂*), 101.61 (C-4a), 112.11 (C-4'), 113.98 (C-2'), 116.45 (C-6'), 117.50 (C-5), 120.50 (C-6), 128.96 (C-5'), 137.16 (C-1'), 148.78 (C-3'), 150.20 (C-2), 152.79 (C-7a), 160.00 ppm (C-4); IR (ATR, neat): $\tilde{v}$ = 3104 (w), 2950 (w), 2855 (w), 2798 (w, 1559 (s), 1502 (m), 1400 (m), 1297 (m), 1228 (w), 1060 (m), 927 (w), 855 (m), 779 (s), 698 (m), 628 cm⁻¹ (s); HR MS (ESI) for $C_{14}H_{16}N_5^+$ [M + H]⁺: calcd 254.1400, found 254.1398.

4-*N,N*-Dimethylamino-5-(3-pyrrolo)-7*H*-pyrrolo[2,3-*d*]pyrimidine (6e)

Compound **5e** (191.8 mg, 0.37 mmol) was subjected to GP1. Purification by HPFC (SiO₂; cHex/EtOAc, gradient 0→100% EtOAc) and repurification (C-18, H₂O/MeOH gradient 5→100% MeOH) gave **6e** (24.3 mg, 29%) as a pale-beige solid.

R_f = 0.34 (SiO₂; EtOAc pure); m.p. = 212–214 °C; ¹H NMR (500 MHz, DMSO-*d₆*): δ = 2.50 (s, 6H; N*Me₂*), 6.16 (m, 1H; H-4'); 6.77 (m, 1H; H-5'); 6.83 (m, 1H; H-2'); 7.09 (d, $J_{6,NH}$ = 2.4 Hz, 1H; H-6), 8.17 (s, 1H; H-2), 10.74 (bs, 1H, N*H*-(H-1')), 11.81 ppm (bs, 1H; N*H*); ¹³C NMR (125.7 MHz, DMSO-*d₆*): δ = 41.20 (N*Me₂*), 103.00 (C-4a), 108.69 (C-4'), 111.44 (C-5), 115.81 (C-2'), 118.00 (C-3' or C-5'), 118.01 (C-5' or C-3'), 119.51 (C-6), 149.79 (C-2), 152.40 (C-7a), 160.70 ppm (C-4); IR (ATR, neat): $\tilde{v}$ = 3197 (w), 3103 (w), 2954 (w), 2858 (w), 1557 (s), 1414 (m), 1404 (m), 1059 (m), 930 (w), 775 (m), 702 (m), 642 (m), 625 cm⁻¹ (m); HR MS (ESI) for $C_{12}H_{14}N_5^+$ [M + H]⁺: calcd 228.1244, found 228.1243.

4-*N,N*-Dimethylamino-7*H*-pyrrolo[2,3-*d*]pyrimidine (6x)[119]
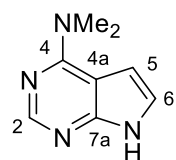
Compound **4** (206.9 mg, 0.49 mmol) was subjected to GP1. After the first purification by HPFC (SiO₂; cHex/EtOAc, gradient 0→100% EtOAc), the obtained compound was stirred at 25 °C in saturated NaHCO₃ for 3 h, then H₂O (30 mL) was added. Extraction by EtOAc (5 × 50 mL) and repurification by HPFC (SiO₂; H₂O/MeOH, gradient 5→100% MeOH) gave **6x** (35.4 mg, 52%) as a pinkish-brown solid.

R_f = 0.52 (SiO₂; EtOAc/MeOH 10:1); m.p. = 217–219°C ([119]: 222 °C); ¹H NMR (500 MHz, DMSO-*d₆*): δ = 3.28 (s, 6H; N*Me₂*), 6.61 (d, $J_{5,6}$ = 3.6 Hz, 1H; H-5); 7.11 (d, $J_{6,5}$ = 3.6 Hz, 1H;

H-6), 8.08 (s, 1H; H-2), 11.59 ppm (bs, 1H; N*H*); ^{13}C NMR (125.7 MHz, DMSO-d_6): δ = 38.80 (N*Me$_2$*), 101.73 (C-5), 102.41 (C-4a), 120.65 (C-6), 150.94 (C-2), 151.58 (C-7a), 152.12 ppm (C-4); IR (ATR, neat): $\tilde{v}$ = 3193 (w), 3096 (w), 2969 (w), 2850 (w), 1566 (s), 1520 (m), 1494 (m), 1400 (m), 13118 (m), 1264 (m), 1056 (m), 924 (m), 820 (m), 719 (s), 680 (m), 623 cm^{-1} (m); HR MS (APCI) for $C_8H_{11}N_4^+$ [M + H]$^+$: calcd 163.0978, found 163.0978.

Table 8 - HPLC purity of final compounds.

Compound	Method	t_r [min]	Purity [%]	Compound	Method	t_r [min]	Purity [%]
6a	B	29.12	96.83	**6c**	B	23.79	95.51
6b	A	30.62	97.54	**6d**	B	26.05	98.32
6by	A	26.00	95.97	**6e**	A	30.29	96.13

Methods: **A**: gradient from 3% MeOH in H$_2$O to 100% MeOH in 50 minutes; **B**: gradient from 3% MeCN in H$_2$O to 100% MeCN in 50 minutes

6. Literature

(1) Bogdanovic, N.; Hansson, O.; Zetterberg, H.; Basun, H.; Ingelsson, M.; Lannfelt, L.; Blennow, K. Alzheimer's disease - the most common cause of dementia. *Läkartidningen*. **2020**, *117*, 1–7.

(2) Centers for Disease Control and Prevention, National Center for Health Statistics. Underlying Cause of Death 1999-2019 on CDC WONDER Online Database, released in 2020. Data are from the Multiple Cause of Death Files, 1999-2019, as compiled from data provided by the 57 vital statistics jurisdictions through the Vital Statistics Cooperative Program. http://wonder.cdc.gov/ucd-icd10.html (accessed Jun 6, 2021).

(3) Alzheimer's Association. 2019 Alzheimer's disease facts and figures. *Alzheimer's Dementia.* **2019**, *15*, 321–387.

(4) Gu, G. J.; Lund, H.; Wu, D.; Blokzijl, A.; Classon, C.; von Euler, G.; Landegren, U.; Sunnemark, D.; Kamali-Moghaddam, M. Role of Individual MARK Isoforms in Phosphorylation of Tau at Ser^{262} in Alzheimer's Disease. *Neuromol. Med.* **2013**, *15*, 458–469.

(5) Annadurai, N.; Agrawal, K.; Džubák, P.; Hajdúch, M.; Das, V. Microtubule affinity-regulating kinases are potential druggable targets for Alzheimer's disease. *Cell. Mol. Life Sci.* **2017**, *74*, 4159–4169.

(6) Alzheimer, A. Über eine eigenartige Erkrankung der Hirnrinde. *Allgemeine Zeitschrift für Psychiatrie und Psychisch-gerichtliche Medizin.* **1907**, *18*, 177–179.

(7) Ulep, M. G.; Saraon, S. K.; McLea, S. Alzheimer Disease. *J. Nurse Pract*. **2018**, *14*, 129–135.

(8) Atri, A. Current and Future Treatments in Alzheimer's Disease. *Semin. Neurol.* **2019**, *39*, 227–240.

(9) Castellani, R. J; Rolston, R.K.; Smith, M. A. Alzheimer disease. *Dis.-Mon*. **2010**, *56*, 484–546.

(10) Fratiglioni, L.; De Ronchi, D.; Aguero-Torres, H. Worldwide prevalence and incidence of dementia. *Drugs Aging.* **1999**, *15*, 365–375.

(11) Shin, H.-Y.; Kim, J.; Lee, S.; Park, M. S.; Park, S.; Huh, S. Cause-of-death statistics in 2018 in the Republic of Korea. *J. Korean Med. Assoc.* **2020**, *63*, 286–297.

(12) Cui, L.; Hou, N.-N.; Wu, H.-M.; Zuo, X.; Lian, Y.-Z.; Zhang, C.-N.; Wang, Z.-F.; Zhang, X.; Zhu, J.-H. Prevalence of Alzheimer's Disease and Parkinson's Disease in China: An Updated Systematical Analysis. *Front. Aging Neurosci.* **2020**, DOI: 10.3389/fnagi.2020.603854.

(13) Karceski, S. The Effects of Long-term Medication Use in Alzheimer Disease. *Neurology*. **2021**, *96*, 2247–2250.

(14) The Alzheimer's Association. ALZHEIMER'S ASSOCIATION REPORT: 2020 Alzheimer's disease facts and figures. *Alzheimer's Dement.* **2020**, *16*, 391–460.

(15) Niu, H.; Alvarez-Alvarez, I.; Guillen-Grima, F.; Aguinaga-Ontoso, I. Prevalence and incidence of Alzheimer's disease in Europe: A meta-analysis. *Neurologia.* **2017**, *32*, 523–532.

(16) Bacigalupo, I.; Mayer, F.; Lacorte, E.; Di Pucchio, A.; Marzolini, F.; Canevelli, M.; Di Fiandra, T.; Vanacore, N. A systematic review and meta-analysis on the prevalence of dementia in europe: Estimates from the highest-quality studies adopting the DSM IV diagnostic criteria. *J. Alzheimers Dis.* **2018**, *66*, 1471–1481.

(17) Prince, M.; Bryce, R.; Albanese, E.; Wimo, A.; Ribeiro, W.; Ferri, C. P. The global prevalence of dementia: a systematic review and metaanalysis. *Alzheimers Dement.* **2013**, *9*, 63–75.

(18) Lladó, A.; Froelich, L.; Khandker, R. K.; Roset, M.; Black, C. M.; Lara, N.; Chekani, F.; Ambegaonkar, B. M. Assessing the Progression of Alzheimer's Disease in Real-World Settings in Three European Countries. *J. Alzheimers Dis.* **2021**, *80*, 749–759.

(19) Brookmeyer, R.; Johnson, E.; Ziegler-Graham, K.; Arrighi, H. M. Forecasting the global burden of Alzheimer's disease. *Alzheimers Dement.* **2007**, *3*, 186–191.

(20) Tellechea, P.; Pujol, N.; Esteve-Belloch, P.; Echeveste, B.; García-Eulate, M. R.; Arbizu, J.; Riverol, M. Early- and late-onset Alzheimer disease: Are they the same entity? *Neurología.* **2018**, *33*, 244–253.

(21) Bird, T.D. Alzheimer Disease Overview. Oct 23, 1998 [updated Dec 20, 2018]. In: Adam, M.P.; Ardinger, H. H.; Pagon, R. A. et al., editors. *GeneReviews®* [Online]. Seattle (WA): University of Washington, Seattle; 1993-2021. https://www.ncbi.nlm.nih.gov/books/NBK1161/ (accessed Apr 19, 2021).

(22) Dorszewska, J.; Prendecki, M.; Oczkowska, A.; Dezor, M.; Kozubski, W. Molecular Basis of Familial and Sporadic Alzheimer's Disease. *Curr. Alzheimer Res.* **2016**, *13*, 952–963.

(23) Liu, C.-C.; Kanekiyo, T.; Xu, H.; Bu, G. Apolipoprotein E and Alzheimer disease: risk, mechanisms, and therapy. *Nat Rev Neurol.* **2013**, *9*, 106–118.

(24) National Center for Biotechnology Information. https://www.ncbi.nlm.nih.gov/gene/348 (accessed Apr 20, 2021).

(25) Gonneaud, J.; Bedetti, C.; Binette, A. P.; Benzinger, T. L. S.; Morris, J. C.; Bateman, R. J.; Poirier, J.; Breitner, J. C. S.; Villeneuve, S. Association of education with Aβ burden in preclinicial familial and sporadic Alzheimer disease. *Neurology.* **2020**, DOI: 10.1212/WNL.0000000000010314.

(26) Tanzi, R. E. The Genetics of Alzheimer Disease. *Cold Spring Harbor Perspect. Med.* **2012**, DOI: 10.1101/cshperspect.a006296.

(27) Bird, T. D.; Sumi, S. M.; Nemens, E. J.; Nochlin, D.; Schellenberg, G.; Lampe, T. H.; Sadovnick, A.; Chui, H.; Miner, G. W.; Tinklenberg, J. Phenotypic heterogeneity in familial alzheimer's disease: A study of 24 kindreds. *Ann. Neurol.* **1989**, *25,* 12–25.

(28) Perry, G.; Cash, A. D.; Smith, M. A. Alzheimer Disease and Oxidative Stress. *J. Biomed. Biotechnol.* **2002**, *2*, 120–123.

(29) Savelieff, M. G.; Lee, S.; Liu, Y.; Lim, M. H. Untangling Amyloid-β, Tau, and Metals in Alzheimer's Disease. *ACS Chem. Biol.* **2013**, *8*, 856−865.

(30) Progress Report on Alzheimer's Disease 2004-2005. *NIH Publ.* **2005**, NIH Publication Number: 05-5724.

(31) Hamley, I. W. The Amyloid Beta Peptide: A Chemist's Perspective. Role in Alzheimer's and Fibrillization. *Chemical Reviews.* **2012,** *112*, 5147–5192.

(32) UniProtKB. https://www.uniprot.org/uniprot/P05067 (accessed Apr 20, 2021).

(33) Colvin, M. T.; Silvers, R.; Ni, Q. Z.; Can, T. V.; Sergeyev, I.; Rosay, M.; Donovan, K. J.; Wall, B. M. J.; Linse, S.; Griffin, R. G. Atomic Resolution Structure of Monomorphic Aβ$_{42}$ Amyloid Fibrils. *J. Am. Chem. Soc.* **2016**, *138*, 9663−9674.

(34) Roher, A. E.; Lowenson, J. D.; Clarke, S.; Woods, A. S.; Cotter, R. J.; Gowing, E.; Ball, M. J. β-Amyloid-(1-42) is a major component of cerebrovascular amyloid deposits: Implications for the pathology of Alzheimer disease. *Proc. Natl. Acad. Sci. U. S. A.* **1993**, *90*, 10836–10840.

(35) Relini, A.; Marano, N.; Gliozzi, A. Misfolding of amyloidogenic proteins and their interactions with membranes. *Biomolecules.* **2014**, *4*, 20–55.

(36) Yan, Y.; Wang, C. Aβ42 is More Rigid than Aβ40 at the C Terminus: Implications for Aβ Aggregation and Toxicity. *J. Mol. Biol.* **2006**, *364*, 853–862.

(37) Chen, Y.-R.; Glabe, C. G. Distinct Early Folding and Aggregation Properties of Alzheimer Amyloid-β Peptides Aβ40 and Aβ42. *STABLE TRIMER OR TETRAMER FORMATION BY Aβ42*. J. Biol. Chem.* **2006**, *281*, 24414–24422.

(38) Wälti, M. A.; Ravotti, F.; Arai, H.; Glabe, C. G.; Wall, J. S.; Böckmann, A.; Güntert, P.; Meier, B. H.; Riek, R. Atomic-resolution structure of a disease-relevant Aβ(1–42) amyloid fibril. *Proc. Natl. Acad. Sci. U.S.A.* **2016**, *113*, 4976–4984.

(39) Selkoe, D. J.; Hardy, J. The amyloid hypothesis of Alzheimer's disease at 25 years. *EMBO Mol. Med.* **2016**, *8*, 595–608.

(40) Relini, A.; Marano, N.; Gliozzi, A. Misfolding of Amyloidogenic Proteins and Their Interactions with Membranes. *Biomolecules.* **2014**, *4*, 20–55.

(41) Mucke, L.; Selkoe, D. J. Neurotoxicity of Amyloidβ-Protein:Synaptic and Network Dysfunction. *Cold Spring Harbor Perspect. Med.* **2012**, DOI: 10.1101/cshperspect.a006338.

(42) Lambert, M. P.; Barlow, A. K.; Chromy, B. A.; Edwards, C.; Freed, R.; Liosatos, M.; Morgan, T. E.; Rozovsky, I.; Trommer, B.; Viola, K. L.; Wals, P.; Zhang, C.; Finch, C. E.; Krafft, G. A.; Klein, W. L. Diffusible, nonfibrillar ligands derived from Ab1-42 are potent central nervous system neurotoxins. *Proc. Natl. Acad. Sci. U.S.A.* **1998**, *95*, 6448–6453.

(43) Goedert, M.; Spillantini, M. G.; Jakes, R.; Rutherford, D.; Crowther, R. A.; Multiple isoforms of human microtubule-associated protein tau: sequences and localization in neurofibrillary tangles of Alzheimer's disease. *Neuron.* **1989**, *3*, 519–526.

(44) National Library of Medicine. National Center for Biotechnology Information. https://www.ncbi.nlm.nih.gov/datasets/tables/genes/?table_type=transcripts&key=a7b93f2d7c96f800f5f7098cb9f98494 (accessed Apr 21, 2021).

(45) Weingarten, M. D.; Lockwood, A. H.; Hwo, S. Y.; Kirschner, M. W. A protein factor essential for microtubule assembly. *Proc. Natl. Acad. Sci. U.S.A.* **1975**, *72*, 1858–1862.

(46) Binder, L. I.; Frankfurter, A.; Rebhun, L. I. The distribution of tau in the mammalian central nervous system. *J. Cell Biol.* **1985**, *101*, 1371–1378.

(47) Tassan, J.-P.; Le Goff, X. An overview of the KIN1/PAR-1/MARK kinase family (Review). *Biol. Cell.* **2004**, *96*, 193–199.

(48) Proteopedia. https://proteopedia.org/wiki/index.php/6cvn (accessed Apr 21, 2021).

(49) Kellogg, E. H.; Hejab, N. M. A.; Poepsel, S.; Downing, K. H.; DiMaio, F.; Nogales, E. Near-atomic model of microtubule-tau interactions. *Science.* **2018**, *360*, 1242–1246.

(50) Lee, V. M.-Y.; Goedert, M.; Trojanowski, J. Q. Neurodegenerative tauopathies. *Annu. Rev. Neurosci.* **2001**, *24*, 1121−1159.

(51) Rosenmann, H.; Blum, D.; Kayed, R.; Ittner, L. M. Tau Protein: Function and Pathology (Editorial). *International Journal of Alzheimer's Disease.* **2012**, DOI: 10.1155/2012/707482.

(52) "Tau phosphorylation site table." From: https://www.kcl.ac.uk/people/diane-hanger (accessed May 24, 2021).

(53) Hampel, H.; Buerger, K.; Zinkowski, R.; Teipel, S. J; Goernitz, A.; Andreasen, N.; Sjoergen, M.; DeBernardis, J.; Kerkman, D.; Ishiguro, K.; Ohno, H.; Vanmechelen, E.; Vanderstichele, H.; McCulloch, C.; Moller, H.-J.;

Davies, P.; Blennow, K. Measurement of Phosphorylated Tau Epitopes in the Differential Diagnosisof Alzheimer Disease: A Comparative Cerebrospinal Fluid Study. *Arch. Gen. Psychiatry.* **2004**, *61*, 95–102.

(54) Iqbal, K.; Grundke-Iqbal, I. Alzheimer neurofibrillary degeneration: significance, etiopathogenesis, therapeutics and prevention. *J. Cell. Mol. Med.* **2008**, *12*, 38–55.

(55) Suárez-Calvet, M.; Karikari, T. K.; Ashton, N. J.; Rodríguez, J. L.; Milà-Alomà, M.; Gispert, J. D.; Salvadó, G.; Minguillon, C.; Fauria, K.; Shekari, M.; Grau-Rivera, O.; Arenaza-Urquijo, E. M.; Sala-Vila, A.; Sánchez-Benavides, G.; González-de-Echávarri, J. M.; Kollmorgen, G.; Stoops, E.; Vanmechelen, E.; Zetterberg, H.; Blennow, K.; Molinuevo, J. L. & for the ALFA Study. Novel tau biomarkers phosphorylated at T181, T217, or T231 rise in the initial stages of the preclinical Alzheimer's continuum when only subtle changes in Aβ pathology are detected. *EMBO Mol. Med.* **2020**, DOI: 10.15252/emmm.202012921.

(56) Wegmann, S.; Biernat, J.; Mandelkow, E. A current view on Tau protein phosphorylation in Alzheimer's disease. *Curr. Opin. Neurobiol.* **2021**, *69*, 131–138.

(57) National Institute of Aging. Treatment of Alzheimer's disease. https://www.nia.nih.gov/health/how-alzheimers-disease-treated (accessed May 24, 2021).

(58) Kato, T.; Satoh, S.; Okabe, H.; Kitahara, O.; Ono, K.; Kihara, C.; Tanaka, T.; Tsunoda, T.; Yamaoka, Y.; Nakamura, Y.; Furukawa, Y. Isolation of a novel human gene, MARKL1, homologous to MARK3 and its involvement in hepatocellular carcinogenesis. *Neoplasia (N.Y., NY, U.S.)* **2001**, *3*, 4–9.

(59) Trinczek, B.; Brajenovic, M.; Ebneth, A.; Drewes, G. MARK4 is a novel microtubule-associated proteins/microtubule affinity-regulating kinase that binds to the cellular microtubule network and to centrosomes. *J. Biol. Chem.* **2004**, *279*, 5915–5923.

(60) Drewes, G.; Ebneth, A.; Preuss, U.; Mandelkow, E.-M.; Mandelkow, E. MARK, a Novel Family of Protein Kinases That Phosphorylate Microtubule-Associated Proteins and Trigger Microtubule Disruption. *Cell.* **1997**, *89*, 297−308.

(61) Lund, H.; Gustaffson, E.; Svensson, A.; Nilsson, M.; Berg, M.; Sunnemark, D.; von Euler, G. MARK4 and MARK3 associate with early tau phosphorylation in Alzheimer's disease granulovacuolar degeneration bodies. *Acta Neuropathol. Commun.* **2014**, DOI: 10.1186/2051-5960-2-22.

(62) Mocanu, M. M.; Nissen, A.; Eckermann, K.; Khlistunova, I.; Biernat, J.; Drexler, D.; Petrova, O.; Schönig, K.; Bujard, H.; Mandelkow, E.; Zhou, L.; Rune, G.; Mandelkow, E.-M. The potential for beta-structure in the repeat domain of tau protein determines aggregation, synaptic decay, neuronal loss, and coassembly with endogenous Tau in inducible mouse models of tauopathy. *J. Neurosci.* **2008**, *28*, 737–748.

(63) Augustinack, J. C.; Schneider, A.; Mandelkow, E. M.; Hyman, B. T. Specific tau phosphorylation sites correlate with severity of neuronal cytopathology in Alzheimer's disease. *Acta Neuropathol.* **2002**, *103*, 26–35.

(64) Biernat, J.; Gustke, N.; Drewes, G.; Mandelkow, E.-M.; Mandelkow, E. Phosphorylation of Ser^{262} strongly reduces binding of tau to microtubules: Distinction between PHF-like immunoreactivity and microtubule binding. *Neuron.* **1993**, *11*, 153–163.

(65) Gustke, N.; Steiner, B.; Mandelkow, E.-M.; Biernat, J.; Meyer, H. E.; Goedert, M.; Mandelkow, E. The Alzheimer-like phosphorylation of tau protein reduces microtubule binding and involves Ser-Pro and Thr-Pro motifs. *FEBS Lett.* **1992**, *307*, 199–205.

(66) Drewes, G. MARKing tau for tangles and toxicity. *Trend Biochem. Sci.* **2004**, *29*, 548–555.

(67) Moroni, R. F.; De Biasi, S.; Colapietro, P.; Larizza, L.; Beghini, A. Distinct expression pattern of microtubule-associated protein/microtubule affinity-regulating kinase 4 in differentiated neurons. *Neurosci.* **2004**, *143*, 83–94.

(68) Sack, J. S.; Gao, M.; Kiefer, S. E.; Myers Jr, J. E.; Newitt, J. A.; Wu, S.; Yan, C. Crystal structure of microtubule affinity-regulating kinase 4 catalytic domain in complex with a pyrazolopyrimidine inhibitor. *Acta Crystallogr. F. Struct. Biol. Commun.* **2016**, *72*, 129−134.

(69) Aneja, B.; Khan, N. S.; Khan, P.; Queen, A.; Hussain, A.; Rehman, T.; Alajmi, M. F.; El-Seedi, H. R.; Ali, S.; Hassan, I.; Abid, M. Design and development of Isatin-triazole hydrazones as potential inhibitors of microtubule affinity-regulating kinase 4 for the therapeutic management of cell proliferation and metastasis. *Eur. J. Med. Chem.* **2019**, *163*, 840–852.

(70) Peerzada, M. N.; Khan, P.; Khan, N. S.; Gaur, A.; Avecilla, F.; Hassan, I.; Azam, A. Identification of morpholine based hydroxylamine analogues: selective inhibitors of MARK4/Par-1d causing cancer cell death through apoptosis. *New J. Chem.* **2020**, *44*, 16626−16637.

(71) Sloman, D. L.; Noucti, N.; Altman, M. D.; Chen, D.; Mislak, A. C.; Szewczak, A.; Hayashi, M.; Warren, L.; Dellovade, T.; Wu, Z.; Marcus, J.; Walker, D.; Su, H.-P.; Edavettal, S. C. Munshi, S.; Hutton, M.; Nuthall, H.; Stanton, M. G. Optimization of microtubule affinity regulating kinase (MARK) inhibitors with improved physical properties. *Bioorg. Med. Chem. Lett.* **2016**, *26*, 4362−4366.

(72) Rosemeyer, H. The Chemodiversity of Purine as a Constituent of Natural Products. *Chem. Biodiversity.* **2004**, *1*, 361−401.

(73) Huang, D.; Zhou, T.; Lafleur, K.; Nevado, C.; Caflisch, A. Kinase selectivity potential for inhibitors targeting the ATP binding site: a network analysis. *Bioinformatics.* **2010**, *26*, 198–204.

(74) Rogne, P.; Rosselin, M.; Grundström, C.; Hedberg, C.; Sauer, U. H.; Wolf-Waltz, M. Molecular mechanism of ATP versus GTP selectivity of adenylate kinase. *PNAS.* **2018**, *115*, 3012–3017.

(75) Veselý, J.; Havlíček, L.; Strnad, M.; Blow, J. J.; Donella-Deana, A.; Pinna, L.; Letham, D. S.; Kato, J.; Detivaud, L.; Leclerc, S.; Meijer, L. Inhibition of cyclin-dependent kinases by purine analogues. *Eur. J. Biochem.* **1994**, *224*, 771–786.

(76) Havlíček, L.; Hanuš, J.; Veselý, J.; Leclerc, S.; Meijer, L.; Shaw, G.; Strnad, M. Cytokinin-Derived Cyclin-Dependent Kinase Inhibitors: Synthesis and cdc2 Inhibitory Activity of Olomoucine and Related Compounds. *J. Med. Chem.* **1997**, *40*, 408–412.

(77) De Azevedo, W. F.; Leclerc, S.; Meijer, L.; Havlíček, L.; Strnad, M.; Kim, S.-H. Inhibition of cyclin-dependent kinases by purine analogues: Crystal structure of human cdk2 complexed with roscovitine. *Eur. J. Biochem.* **1997**, *243*, 518–526.

(78) Stýskalová, L.; Cwiertka, K.; Nosková, V.; Janošťáková, A.; Radová, L.; Mihál, V.; Hajdúch, M. CYTOTOXICKÁ AKTIVITA BOHEMINU IN VITRO NA PRIMÁRNÍCH NÁDOROVÝCH BUŇKÁCH. *Klin. Farmakol. Farm.* **2006**, *20*, 197–201.

(79) Hajdúch, M.; Havlíček, L.; Veselý, J.; Novotný, R.; Mihál, V.; Strnad, M. Synthetic Cyclin Dependent Kinase Inhibitors. In *Drug Resistance in Leukemia and Lymphoma III*, Advances in Experimental Medicine and Biology series **1999***; 457*, 341–353.

(80) Raynaud, F. I.; Whittaker, S. R.; Fischer, P. M.; McClue, S.; Walton, M. I.; Barrie, S. E.; Garrett, M. D.; Rogers, P.; Clarke, S. J.; Kelland, L. R.; Valenti, M.; Brunton, L.; Eccles, S.; Lane, D. P.; Workman, P. *In vitro* and *In vivo* Pharmacokinetic-Pharmacodynamic Relationships for the Trisubstituted Aminopurine Cyclin-Dependent Kinase Inhibitors Olomoucine, Bohemine and CYC202. *Clin. Cancer Res.* **2005**, *11*, 4875−4888.

(81) Strnad, M. Kryštof, R. V.; Havlíček, L.; Swaczynova, J. New anticancer drugs derived from plant hormones. *Planta Med.* **2008**, DOI: 10.1055/s-0028-1083914.

(82) Sava, G. P.; Fan, H.; Coombes, R. C.; Buluwela, L.; Ali, S. CDK7 inhibitors as anticancer drugs. *Cancer Metastasis Rev.* **2020**, *39*, 805–823.

(83) Alsfouk, A. A.; Alshibl, H. M.; Altwaijry, N. A.; Alsfouk, B. A.; Al-Abdullah, E. S. Synthesis and biological evaluation of seliciclib derivatives as potent and selective CDK9 inhibitors for prostate cancer therapy. *Monatsh. Chem.* **2021**, *152*, 109–120.

(84) Nishimura, H.; Katagiri, K.; Sato, K.; Mayama, M.; Shimaoka, N. Toyocamycin, a new anti-candida antibiotics. *J. Antibiot. (Tokyo)* **1956**, *9*, 60−62.

(85) Anzai, K.; Nakamura, G.; Suzuki, S. A new antibiotic, tubericidin. *J. Antibiot. (Tokyo)* **1957**, *10*, 201−204.

(86) Rao, K. V.; Renn, D. W. BA-90912: An antitumor substance. *Antimicrob. Agents Chemother.* **1963**, *161*, 77−79.

(87) McCarty, R. M.; Bandarian, V. Biosynthesis of pyrrolopyrimidines. *Biooorg. Chem.* **2012**, *43*, 15–25.

(88) Perlíková, P.; Hocek, M. Pyrrolo[2,3-*d*]pyrimidine (7-deazapurine) as a privileged scaffold in design of antitumor and antiviral nucleosides. *Med. Res. Rev.* **2017**, *37*, 1429−1460.

(89) Fraser, C.; Dawson, J. C.; Dowling, R.; Houston, D. R.; Weiss, J. T.; Munro, A. F.; Muir, M.; Harrington, L.; Webster, S. P.; Frame, M. C.; Brunton, V. G.; Patton, E. E.; Carragher, N. O.; Unciti-Broceta, A. Rapid Discovery and Structure–Activity Relationships of Pyrazolopyrimidines That Potently Suppress Breast Cancer Cell Growth via SRC Kinase Inhibition with Exceptional Selectivity over ABL Kinase. *J. Med. Chem.* **2016**, *59*, 4697–4710.

(90) Tandon, M.; Johnson, J.; Li, Z.; Xu, S.; Wipf, P.; Wang, Q. J. New Pyrazolopyrimidine Inhibitors of Protein Kinase D as Potent Anticancer Agents for Prostate Cancer Cells. *PLOS ONE* **2013**, DOI: 10.1371/journal.pone.0075601.

(91) Mohamed, M. S.; Sayed, A. I.; Khedr, M. A.; Soror, S. H. Design, synthesis, assessment, and molecular docking of novel pyrrolopyrimidine (7-deazapurine) derivatives as non-nucleoside hepatitis C virus NS5B polymerase inhibitors. *Bioorg. Med. Chem.* **2016**, *24*, 2146–2157.

(92) Lawhorn, B. G.; Philip, J.; Zhao, Y.; Louer, C.; Hammond, M.; Cheung, M.; Fries, H.; Graves, A. P.; Shewchuk, L.; Wang, L.; Cottom, J. E.; Qi, H.; Zhao, H.; Totoritis, R.; Zhang, G.; Schwartz, B.; Li, H.; Sweitzer, S.; Holt, D. A.; Gatto Jr., G. J.; Kallander, L. S. Identification of Purines and 7-Deazapurines as Potent and Selective Type I Inhibitors of Troponin I-Interacting Kinase (TNNI3K). *J. Med. Chem.* **2015**, *58*, 7431–7448.

(93) Balasubramanian, P. K.; Balupuri, A.; Bhujbal, S. P.; Cho, S. J. 3D-QSAR Assisted Design of Novel 7-Deazapurine Derivatives as TNNI3K Kinase Inhibitors Using Molecular Docking and Molecular Dynamics Simulation. *Lett. Drug Des. Discovery* **2020**, *17*, 155−168.

(94) Henderson, J. L.; Kormos, B. L.; Hayward, M. M.; Coffman, K. J.; Jasti, J.; Kurumbail, R. G.; Wager, T. T.; Verhoest, P. R.; Noell, G. S.; Chen, Y.; Needle, E.; Berger, Z.; Steyn, S. J.; Houle, C.; Hirst, W. D.; Galatsis, P. Discovery and preclinical profiling of 3-[4-(morpholin-4-yl)-7H-pyrrolo[2,3-d]pyrimidin-5-yl]benzonitrile (PF-06447475), a highly potent, selective, brain penetrant, and in vivo active LRRK2 kinase inhibitor. *J. Med. Chem.* **2015**, *58*, 419–432.

(95) Galatsis, P.; Hayward, M. M.; Henderson, J.; Kormos, B. L.; Kurumbail R. G.; Stepan, A. F.; Verhoest, P. R.; Wager, T. T.; Zhang, L. NOVEL-4-(SUBSTITUTED -AMINO)-7H-PYRROLO[2,3-d]PYRIMIDINES AS LRRK2 INHIBITORS. WO 2014/001973 A1, January 3, 2014.

(96) Klečka, M.; Poštová Slavětínská, L.; Tloušťová, E.; Džubák, P.; Hajdúch, M.; Hocek, M. Synthesis and cytostatic activity of 7-arylsulfanyl-7-deazapurine bases and ribonucleosides. *Med. Chem. Commun.* **2015**, *6*, 576–580.

(97) Sabat, N.; Smoleń, S.; Nauš, P.; Perlíková, P.; Cebová, M.; Poštová Slavětínská, L.; Hocek, M. Synthesis of 2,6-Substituted 7-(Het)aryl-7-deazapurine Nucleobases (2,4-Disubstituted 5-(Het)aryl-pyrrolo[2,3-d]pyrimidines). *Synthesis* **2017**, *49*, 4623−4650.

(98) Gerber, P. R.; Müller, K. MAB, a Generally Applicable Molecular Force Field for Structure Modelling in Medicinal Chemistry. *J. Comput. Aided Mol. Des.* **1995**, *9*, 251−268.

(99) Protein Data Bank. https://www.rcsb.org/structure/5ES1 (accessed Jun 7, 2021).

(100) Miyaura, N.; Yamada, K.; Suzuki, A. A new stereospecific cross-coupling by the palladium-catalyzed reaction of 1-alkenylboranes with 1-alkenyl or 1-alkynyl halides. *Tetrahedron Lett.* **1979**, *20*, 3437−3440.

(101) The Nobel Prize in Chemistry 2010. https://www.nobelprize.org/prizes/chemistry/2010/summary/ (accessed Jun 14, 2021).

(102) Miyaura, N.; Suzuki, A. Palladium-Catalyzed Cross-Coupling Reactions of Organoboron Compounds. *Chem. Rev.* **1995**, *95*, 2457–2483.

(103) Chemler, S. R.; Trauner, D.; Danishefsky, S. J. The B-Alkyl Suzuki-Miyaura Cross-Coupling Reaction: Development, Mechanistic Study, and Applications in Natural Product Synthesis. *Angew. Chem. Int. Ed.* **2001**, *40*, 4544–4568.

(104) Suzuki, A. Recent advances in the cross-coupling reactions of organoboron derivatives with organic electrophiles, 1995 − 1998. *J. Orgmet. Chem.* **1999**, *276*, 147−168.

(105) Littke, A. F.; Dai, C.; Fu, G. C. Versatile Catalysts for the Suzuki Cross-Coupling of Arylboronic Acids with Aryl and Vinyl Halides and Triflates under Mild Conditions. *J. Am. Chem. Soc.* **2000**, *122*, 4020–4028.

(106) Miyaura, N.; Ishiyama, T.; Sasaki, H.; Ishikawa, M.; Satoh, M.; Suzuki, A. Palladium-catalyzed inter- and intramolecular cross-coupling reactions of B-alkyl-9-borabicyclo[3.3.1]nonane derivatives with 1-halo-1-alkenes or haloarenes. Syntheses of functionalized alkenes, arenes, and cycloalkenes via a hydroboration-coupling sequence. *J. Am. Chem. Soc.* **1989**, *111*, 314–321.

(107) Bedford, R. B.; Welch, S. L. Palladacyclic phosphinite complexes as extremely high activity catalysts in the Suzuki reaction. *Chem. Commun.* **2001**, *1*, 129−130.

(108) Suzuki, A. Organoborane coupling reactions (Suzuki coupling). *Proc. Jpn. Acad.* **2008**, *80*, 359−371.

(109) Dupuis, C.; Adiey, K.; Charruault, L,; Michelet, V.; Savignac, M.; Gênet, J.-P. Suzuki cross-coupling of arylboronic acids mediated by ahydrosoluble Pd(0)/TPPTS catalyst. *Tetrahedron Lett.* **2001**, *42*, 6523–6526.

(110) Song, Y.; Ding, X.; Dou, Y.; Yang, R.; Sun, Q.; Xiao, Q.; Ju, Y. Efficient and Practical Synthesis of 5′-Deoxytubercidin and Its Analogues via Vorbrüggen Glycosylation. *Synthesis* **2011**, *155*, 1442−1446.

(111) Reiersølmoen, A. C.; Han, J.; Sundby, E.; Hoff, B. H. Identification of fused pyrimidines as interleukin 17 secretion inhibitors. *Eur. J. Med. Chem.* **2018***, 155,* 562–578.

(112) Fleuti, M.; Bártová, K.; Poštová Slavětínská, L.; Tloušťová, E.; Tichý, M.; Gurská, S.; Pavliš, P.; Džubák, P.; Hajdúch, M.; Hocek, M. Synthesis and Biological Profiling of Pyrazolo-Fused 7-Deazapurine Nucleosides. *J. Org. Chem.* **2020**, *85*, 10539−10551.

(113) Ahmadi, Z.; McIndoe, J. S. A mechanistic investigation of hydrodehalogenation using ESI-MS. *Chem. Commun.* **2013**, *49*, 11488−11490.

(114) Jedinák, L.; Zátopková, R.; Zemánková, H.; Šustková, A.; Cankař, P. The Suzuki–Miyaura Cross-Coupling Reaction of Halogenated Aminopyrazoles: Method Development, Scope, and Mechanism of Dehalogenation Side Reaction. *J. Org. Chem.* **2017**, *82*, 157–169.

(115) Miles, D. H.; Yan, X.; Thomas-Tran, R.; Fournier, J.; Sharif, E. U.; Drew, S. L.; Mata, G.;Lawson, K. V.; Ginn, E.; Wong, K.; Soni, D.; Dhanota, P.; Shaqfeh, S. G.; Meleza, C.; Chen, A.; Pham, A. T.; Park, T.; Swinarski, D.; Banuelos, J.; Schindler, U.; Walters, M. J.; Walker, N. P.; Zhao, X.; Young, S. W.; Chen, J.; Jin, L.; Leleti, M.

R.; Powers, J. P.; Jeffrey, J. L. Discovery of Potent and Selective 7-Azaindole Isoindolinone-Based PI3Kγ Inhibitors. *ACS Med. Chem. Lett.* **2020**, *11*, 2244−2252.

(116) Rodgers, J. D.; Shepard, S.; Maduskuie Jr., T. P.; Wang, H.; Falahatpisheh, N.; Rafalski, M.; Arvanitis, A. G.; Storace, L.; Jalluri, R. K.; Fridman, J. S.; Vaddi, K. HETEROARYL SUBSTITUTED PYRROLO[2,3-B]PYRIMIDINES AND PYRROLO[2,3-B]PYRIMIDINES AS JANUS KINASE INHIBITORS. US 20070135461 A1, June 14, 2007.

(117) Shen, X.; Liu, X.; Wan, S.; Fan, X.; He, H.; Wei, R.; Pu, W.; Peng, Y.; Wang, C. Discovery of Coumarin as Microtubule Affinity-Regulating Kinase 4 Inhibitor That Sensitize Hepatocellular Carcinoma to Paclitaxel. *Front. Chem.* **2019**, DOI: 10.3389/fchem.2019.00366.

(118) Lategahn, J.; Hardick, J.; Grabe, T.; Niggenaber, J.; Jeyakumar, K.; Keul, M.; Tumbrink, H. L.; Becker, C.; Hodson, L.; Kirschner, T.; Klövekorn, F.; Ketzer, J.; Baumann, M.; Terheyden, S.; Weisner, A. U. J.; Müller, M. P.; van Otterlo, W. A. L.; Bauer, S.; Rauh, D. Targeting Her2-insYVMA with Covalent Inhibitors − A Focused Compound Screening and Structure-Based Design Approach. *J. Med. Chem.* **2020**, *63*, 11725−11755.

(119) Wellcome Foundation Ltd. Pyrrolo[2,3-d]Pyrimidine Derivatives and the manufacture thereof. GB 915303 A, January 9, 1963.